Journal of the OPTICAL SOCIETY *of* AMERICA

VOLUME 28
No. 9

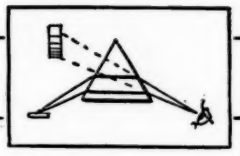

SEPTEMBER
1938

Apparatus for Testing Highway Sign Reflector Units . . . . . R. KINGSLAKE 323

Path of a Ray of Light Tangent to the Surface of the Earth . . . . . JOHN SWEER 327

Correlation of Optical Properties and Photoelectric Emission in Thin Films of Alkali Metals . . . . . HERBERT E. IVES AND H. B. BRIGGS 330

Further Search for the Ideal Color System II. A Reconsideration of the Helmholtz Line Element . . . . . R. H. SINDEN 339

Surrounding Gaseous Medium and the Herschel Effect . . . . . MARLIN THURSTON AND JULIAN M. BLAIR 348

Physical Density Comparator . . . . . MONROE HAMILTON SWEET 349

Published monthly
at Prince and Lemon Sts., Lancaster, Pa.
by the
AMERICAN INSTITUTE OF PHYSICS
Incorporated
175 Fifth Avenue, New York, N. Y.
FOR AND UNDER THE EDITORIAL SUPERVISION OF
THE OPTICAL SOCIETY OF AMERICA

BOSTON UNIVERSITY
COLLEGE OF LIBERAL ARTS
LIBRARY

THE OPTICAL SOCIETY OF AMERICA

Officers of the Society

R. C. GIBBS, *President*
Cornell University
Ithaca, New York

K. S. GIBSON, *Vice President*
National Bureau of Standards
Washington, D. C.

L. B. TUCKERMAN, *Secretary*
National Bureau of Standards
Washington, D. C.

HENRY F. KURTZ, *Treasurer*
Bausch & Lomb Optical Company
Rochester, New York

The Board of Directors consists of the above officers; the Editor of the Journal; the Past President; and five directors-at-large.

A. C. HARDY, *Past President*
Massachusetts Institute of Technology
Cambridge, Massachusetts

F. K. RICHTMYER, *Editor*
Cornell University
Ithaca, New York

Directors-at-Large

H. P. GAGE
Corning Glass Works
Corning, New York

G. R. HARRISON
Massachusetts Institute of Technology
Cambridge, Massachusetts

WILLIAM F. MEGGERS
National Bureau of Standards
Washington, D. C.

BRIAN O'BRIEN
University of Rochester
Rochester, New York

A. G. WORTHING
University of Pittsburgh
Pittsburgh, Pennsylvania

Rochester, New York, Section of the Optical Society of America

A. A. COOK, *President* H. E. SEEMANN, *Vice President* J. H. WEBB, *Secretary* H. F. SHERWOOD, *Treasurer*
Councillors: S. W. BARNES, R. E. BURROUGHS, K. J. HEINICKE, F. H. PERRIN, B. NOYES (*ex officio*)

Corporation Members of the Optical Society of America

American Optical Company, Southbridge, Massachusetts
Bausch & Lomb Optical Company, Rochester, New York
Bell Telephone Laboratories, Inc., New York, New York
Corning Glass Works, Corning, New York
Gaertner Scientific Corporation, Chicago, Illinois
Interchemical Corporation, New York, New York
Keuffel & Esser Company, Hoboken, New Jersey
Spencer Lens Company, Buffalo, New York
Arthur H. Thomas Company, Philadelphia, Pennsylvania

THE OPTICAL SOCIETY OF AMERICA was organized in 1916 "*to increase and diffuse the knowledge of optics in all its branches, pure and applied, to promote the mutual interests of investigators of optical problems, of designers, manufacturers and users of optical instruments and apparatus of all kinds and to encourage cooperation among them.*" It aims to serve the interests of all who are engaged in any branch of optics from fundamental research to the manufacture of optical goods.

MEMBERSHIP

Regular Members: "Any person who has contributed materially to the advancement of optics is eligible for regular membership."

Associate Members: "Any person who is interested in optics is eligible for associate membership."

Corporate Members: "Any corporation desirous of encouraging the work of the Society is eligible for corporation membership."

The Society cordially invites to membership all who are interested in any branch of optics, either in research, in instruction, in optical or illuminating engineering, in the manufacture and distribution of optical goods of all kinds or in physiological and medical optics.

ANNUAL DUES

Regular members, $7.50; Associate members, $5.00; Corporate members, $50.00. These dues include subscription to the Society's official journal, the *Journal of the Optical Society of America.*

MEETINGS

The Society holds two meetings per year: An annual meeting in the autumn and a midwinter meeting jointly with the American Physical Society.

For further information concerning the Optical Society of America address the Secretary, Dr. L. B. Tuckerman, National Bureau of Standards, Washington, D. C.

Journal of the
OPTICAL SOCIETY
of AMERICA

VOLUME 28 SEPTEMBER, 1938 NUMBER 9

An Apparatus for Testing Highway Sign Reflector Units

R. KINGSLAKE
Institute of Applied Optics, University of Rochester, Rochester, New York
(Received July 2, 1938)

THERE appears to be some demand for a better method of measuring the reflecting power of the familiar lens-mirror reflector units (so-called "buttons") used in highway signs and warnings. At present, these units are generally tested by the rather primitive and unsatisfactory procedure of merely erecting a number of the units at the side of a straight road, and making a visual observation of their brightness when illuminated by an automobile headlamp.

A number of attempts have been made to devise laboratory tests for buttons, the most successful being those in which the apparent brightness of an illuminated button is compared visually with the brightness of a disk of opal glass illuminated from behind by a lamp of variable intensity.[1] The objections to this kind of test are that the apparatus is not conveniently portable, a long room or laboratory is required, and the observations are of a kind in which good repetitions of readings are difficult to secure. However, such simple tests, though necessarily inaccurate, are convincing to an unscientific observer, and they can be readily adapted to determine the apparent brightness of the unit at different angles from the axis and for different angles of incidence of the light falling on it. In some forms of laboratory test designed for use in a compact space, the results are liable to be misleading as the light falling on the button is not parallel.

[1] This type of test was adopted in 1932 in the *Joint I.E.S.–S.A.E. Standard Specification for Laboratory Tests of Reflex Reflectors for Motor Vehicles*, obtainable from the Illuminating Engineering Society, 51 Madison Avenue, New York City. This specification requires that the reflector shall be tested at 100 feet from a headlamp of 10,000 candlepower, thus providing an illumination of 1 foot-candle on the reflector. The apparent candlepower of the reflector is then measured by an observer situated 7 inches (one-third of a degree) above the center of the headlamp.

THE CONDITIONS TO BE FULFILLED BY A SATISFACTORY REFLECTING UNIT

Before describing the proposed testing apparatus, it might be useful to point out some of the properties of a reflecting unit of the type under consideration, and to indicate the practical requirements which must be met by such a unit.

It is the function of a button to reflect light back towards the source from which it comes, but it is obvious that there must be some spreading of the reflected light in order to reach the eyes of the driver of the vehicle. For example, if the driver's eye is 24 inches above the line joining the headlamp to the button, the angular spread required for the button to be visible is given in Table I. It will be clear that this spread should be kept as small as possible in order to conserve light, and it is found that if the greatest care is taken in the design and manufacture of a button, it is actually possible to reduce the spread to such a small amount that most of the reflected light

TABLE I.

Car to button distance (ft.)	1000	500	200	100	50	20
Required spread	0° 7′	0° 14′	0° 34′	1° 8′	2° 17′	5° 43′

will be concentrated within a cone having an angle of only one or two degrees about the axis of the incident light. In such a case there will be very little light scattered beyond about one degree, and as will be seen from Table I, such a button would appear fully bright only when seen at a considerable distance from the vehicle. On the other hand, when such a button is viewed by a close vehicle there is a compensation because the headlamp illumination falling on the button is then greater, so that in spite of the reduced reflecting power, a button of this kind may often be used at quite close distances.

Since in practice it is necessary to see a button at about 1000 feet, and to read the sign itself between 200 feet and 50 feet, and because of this compensation at close distances, we may say that to be satisfactory for highway use, a button should reflect most of the incident light into a cone of about 1° angle. This angle is not at all a definite quantity on account of the wide variation in the practical conditions under which buttons are used, but it represents a fair compromise between the various factors involved.

We have so far considered the action of a button when the incident light falls upon it axially, but since the sign carrying the buttons must be erected at a short distance to one side of the highway, it is evident that the incident light may come from directions which are considerably inclined to the axis of the button, especially when the vehicle is fairly close to the sign. For this reason, the concave mirror inside the reflecting unit is generally made large enough to give reflection up to obliquities of 40° or so from the axis of the button. However, beyond about 10° the oblique astigmatism in the lens causes a progressively increasing spread of the reflected beam, and the button therefore appears continually dimmer as the obliquity is increased beyond 10°. For example, if a sign is placed at 15 feet to one side of the path of an automobile, the face of the sign being at right angles to the roadway, the obliquity of the light falling on the button will vary with the distance of the car in the manner indicated in Table II.

These angles will of course be completely changed if the whole sign is turned somewhat relative to the direction of the highway, and a button must therefore give good reflection over an obliquity range of at least 15° from the axis, and some reflection out to 35° or 40° from the axis. It is fortunate that these high obliquities occur only when the vehicle is close to the sign and when less reflection is required for the sign to be visible. Against this is the fact that when the vehicle is close up to the sign, the main beam of the headlamps may miss the sign altogether, and the reflectors would then receive very little light.

A PORTABLE TESTING APPARATUS

To test how closely a given button fulfils these conditions, and to overcome the difficulties which are encountered in other forms of test, a compact apparatus has been constructed in which parallel light is supplied to the button, and the amount of reflected light is measured by a photoelectric cell. The essential idea of the apparatus is that light diverging from a small hole drilled in a barrier-layer cell,[2] after collimation by a lens, is allowed to fall upon the button under test, and thence is reflected back on to the sensitive face of the cell. The arrangement is shown in Fig. 1. In this figure, L represents a 200-watt projection lamp, and C is a condensing lens to form an

TABLE II.

Distance (ft.)	1000	500	200	100	50	20
Obliquity	1°	2°	4°	8°	17°	37°

image of the lamp filament on the small hole in the photo-cell P. The collimator lens is at T, and B is the unit under test. It is clear that an optically flat mirror placed at B would form an image of the hole alongside the hole itself at P,

[2] An "electrocell" was used in this apparatus, coupled directly to a 0–20 microammeter. Care was taken in drilling the hole to avoid any burr which might short-circuit the cell. The suggestion to drill the photo-cell in this manner was made to the author by Mr. Clifton Tuttle.

and an optically perfect cube-corner prism or triple mirror placed at B would reflect all the light back into the hole at P, thus giving a zero reading on the microammeter M. Since such a perfect reflector would not be suitable for highway purposes, it is very reasonable that the meter should give a low or zero reading for it.

An ordinary reflector button placed at B will send most of the light back towards the hole at P, but on account of the spreading action of

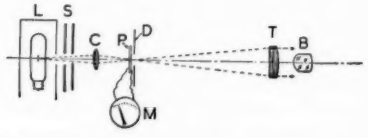

FIG. 1. Schematic arrangement of button testing apparatus.

such a unit, the light will be distributed over a more or less uniform patch on the face of the cell surrounding the hole. Since as we have seen, a good button should reflect most of the light within a 1° cone, it is desired to restrict the measurement to the light within that cone, and to reject all light falling outside it. This is done by covering the photo-cell with a diaphragm D containing an aperture concentric with the original hole P, the aperture having a radius which subtends 1° at the center of the objective T. Thus as T has a focal length of 28 cm, the diaphragm aperture must have a diameter of 1 cm.

As regards the size of the hole drilled in the cell, this should correspond to the diameter of an automobile headlamp. An 8-inch lamp at 100 feet distance subtends about 0° 23′, and to represent this case, the hole in the cell should have a diameter of 1.9 mm. In the present apparatus, a hole of this size was found to transmit so little light that it was widened to 3 mm diameter. The hole now subtends about 0° 37′ at the collimator lens, which is probably quite satisfactory in practice. This corresponds to the angle subtended by an 8-inch headlamp at a distance of 62 feet.

If a number of buttons of different sizes or different qualities are placed in succession at B, the meter reading in each case will provide a direct measure of the reflecting power of the button, within the conditions stated. If it is desired to measure the amount of light reflected into cones of angle other than 1°, the appropriate diaphragm can be placed in front of the cell at D.

It is most necessary to avoid fatigue and overheating of the cell. To prevent this, two asbestos screens are mounted between the lamp housing and the condenser lens, at S in Fig. 1, and a piece of plate glass is inserted in the beam to absorb some further heat. Also, a simple shutter is fitted between the lamp and the condenser, which is normally kept closed and is opened only during the 3 or 4 seconds required to make a reading on a button. With these precautions, the reading given by the same button remains practically constant over a working period of several hours. A ballast tube may be used in series with the lamp to ensure constancy of lamp brightness in spite of fluctuations in the line voltage.

It is necessary to calibrate the cell, since the current from a barrier-layer photo-cell is not proportional to the illumination except at very low illuminations. This calibration may be made by placing a given lamp at a succession of known distances from the cell, and noting the meter reading at each position. A calibration curve can then be drawn connecting the meter reading with the illumination on the cell. The illumination may be expressed in arbitrary units such that the lower readings correspond exactly with the meter reading in microamperes. For the cell used, the calibration was found to be as given in Table III.

To compare the absolute efficiencies of buttons of different sizes, the cell illumination given by each should be divided by the area of the button. However, in comparing the ultimate effectiveness of various buttons, no correction for area should be made because a larger button gives a higher meter reading and also appears brighter when actually in use.

It should be mentioned that the meter shows a low reading (0.9 microamp.) when no button is placed in the beam. This is due to light scattered by the rim of the hole in the cell, and light reflected back from the two faces of the collimating lens. This zero reading should of course be subtracted from all readings to obtain a significant comparison between the reflecting powers of different buttons.

TABLE III.

METER RDG. (μa)	2	4	6	8	10	12	14	16	18	20
Cell illumination (arbitrary units)	2	4	6	8.1	10.3	13.0	16.1	19.6	23.4	27.6

Some typical series of measurements on actual buttons, selected haphazardly, gave the following figures (Table IV). Some of the types tested had separate metal mirrors, and in some the mirror was formed directly on the rear of the thick lens. It has been found that road tests on buttons which have been tested with this apparatus entirely confirm the relative reflecting powers so measured. The zero reading has been deducted from all the figures given here.

Buttons may be tested in this apparatus under any desired angle of incidence by merely turning the button through the required angle about a convenient axis. It is often found that the reflected light is somewhat more concentrated when the angle of incidence is two or three degrees away from the axis of the button than when the incident light is truly axial. This condition causes a slight increase in the meter reading when the button is slightly tilted, but the reading then drops as the button is tilted to greater angles. The average meter readings ob-

TABLE IV.

MANUFACTURER	DIAMETER OF BUTTON APERTURE (MM)	NO. OF BUTTONS TESTED	METER READINGS		
			AVERAGE	LOWEST	HIGHEST
A	20	11	6.6	5.5	8.1
A	17.5	12	7.0	5.3	8.2
A	14.5	20	4.3	3.1	5.6
A	6.5	6	0.6	0.5	0.8
B	20	24	6.0	4.2	7.1
B	15	30	2.5	2.0	3.8
C	20	20	4.4	3.0	6.1
D	24	3	3.8	3.6	4.1

TABLE V.

OBLIQUITY	0	5°	10°	15°	20°	25°	30°	35°	40°	45°	50°	55°
Type 1	6.4	6.3	5.6	5.0	4.0	3.2	2.4	1.7	1.1	0.8	0.2	0
Type 2	7.1	7.1	6.9	6.3	4.6	2.6	2.0	1.1	0.1	0		

tained with several buttons of each of two different types are given in Table V.

In practice this apparatus is found to be very quick and easy to use, about four seconds being sufficient time to make a single test on any given button. If the various parts were rigidly mounted in a suitable light metal box, a convenient portable apparatus could be constructed for routine or comparison testing of buttons in factories and highway engineers' laboratories.

THE RELATION BETWEEN READINGS GIVEN BY THIS APPARATUS, AND THE DIRECT MEASUREMENT OF CANDLEPOWER

Such a correlation is hard to obtain since the meter reading obtained with this apparatus is a measure of the total flux sent by the button into a certain narrow cone, while tests depending on a direct candlepower measurement give the intensity of the button in one specified direction only. Thus the reading given by the present instrument is an integration of the flux reflected into all directions within the specified cone, while the other type of test measures the light reflected into one direction only. Nevertheless, both types of test are equally valid for comparison purposes, the advantages of the present apparatus being portability and compactness, the extreme ease and rapidity with which a test may be made, and the fact that no visual photometric match is required. Moreover, if the button should scatter light somewhat irregularly into different directions, the photo-cell serves to give the average intensity directly.

The Path of a Ray of Light Tangent to the Surface of the Earth

JOHN SWEER
Naval Research Laboratory, Washington, D. C.
(Received June 17, 1938)

The general equations of the path of a ray of light passing through the terrestrial atmosphere are outlined. The path of the ray tangent to the earth's surface is calculated for the U. S. Standard Atmosphere. From this is prepared a table of horizon dip, horizon distance, and refraction for altitudes from sea level to 100,000 feet.

THE path of a ray of light tangent to the earth at its surface has been determined by McLeod[1] for heights up to about 50,000 feet, using the values of atmospheric density in the *Computer's Handbook*.[2] Because of the bearing of such a computation on problems of meteorological optics and stratospheric navigation without an artificial horizon, it is useful to know the path to greater heights. The present report gives a table and curves of the dip of the horizon, the distance to the horizon, and the net refraction from sea level to 100,000 feet, above which the refraction is negligible. Formulae are included for extending the table to higher altitudes and for modifications due to the different indices of refraction of light of various wave-lengths. The atmospheric densities used were those of the U. S. Standard Atmosphere.[3]

Let disturbances originating at two points z_1 and z_2, Fig. 1, separated by a distance s on the wave front AB be propagated in a medium whose refractive index μ is a function only of the altitude z. Let ϕ be the zenith angle of the wave normal. At some later time, the disturbances will have advanced by amounts r_1 and r_2, where

$$r_1/r_2=\mu_2/\mu_1,$$

the subscripts referring to the values at the respective points. The new wave front A_1B_1 will then have changed in direction by an amount $d\phi$, where

$$d\phi=\arcsin(r_2-r_1)/s.$$

Then
$$\sin(d\phi)=r_1(\mu_1-\mu_2)/s\mu_2,$$
$$=-r_1(d\mu/dz)(z_2-z_1)/s[\mu_1+(d\mu/dz)(z_2-z_1)],$$
$$=-r_1\sin\phi(d\mu/dz)/[\mu_1+(d\mu/dz)(z_2-z_1)].$$

As we take the points z_1 and z_2 closer together, $z_2-z_1\to 0$, $\sin(d\phi)\to d\phi$, and

$$d\phi/dz=-\tan\phi[d\mu/dz]/\mu, \qquad (1)$$

where $r_1\cos\phi=dz$, the change in height of the ray.

The zenith angle of a ray going through the atmosphere will change with height not only because of refraction, but also because of the curvature of the earth. Assuming a spherical earth, we write as the differential equation to be satisfied by each point of the ray path

$$d\phi=-\frac{d\mu}{\mu}\tan\phi-\frac{\tan\phi}{R+z}dz,$$

where R is the radius of the earth and z is the height of the point. Then

$$\log\sin\phi=-\log\mu-\int\frac{dz}{R+z}$$
$$=-\log\mu(R+z)+\text{const.},$$

or more simply

$$\sin\phi=A/(R+z)\mu,$$

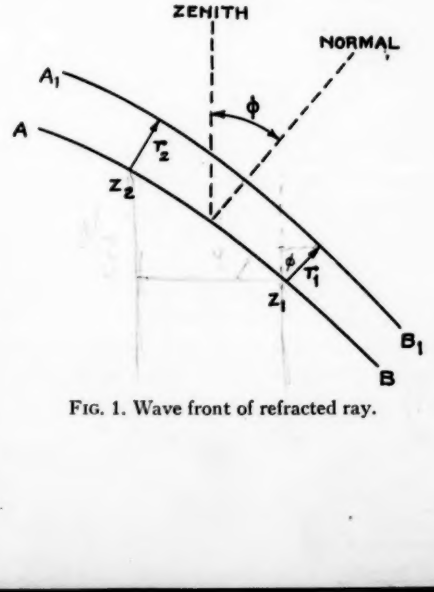

FIG. 1. Wave front of refracted ray.

[1] A. R. McLeod, Phil. Mag. **38**, 546 (1919).
[2] Meteorological Publication, M.O. 223.
[3] W. G. Brombacher, NACA Report No. 538 (1935).

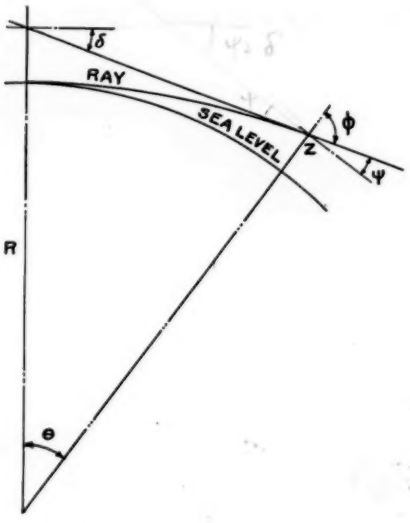

FIG. 2. Ray in terrestrial atmosphere.

where A is a constant for any given ray, determined only by the ray's initial zenith angle and the index of refraction at sea level.

We are concerned with the ray tangent to the earth's surface. In this case $\phi=\pi/2$ and $A=R\mu_0$, where μ_0 is the refractive index of the atmosphere at sea level. Whence

$$\sin\phi=R\mu_0/(R+z)\mu. \tag{2}$$

By Dale and Gladstone's law,

$$\mu=1+a\rho, \tag{3}$$

where ρ is proportional to the density of the air and a is a constant for a given wave-length of light. We take

$$\rho=\frac{P/T}{P/T|_{z=0}},$$

where P is the pressure and T is the temperature of the air, thus making $a=0.000277$ for $\lambda 5800$ at 15°C and 760 mm of mercury.

The horizon dip ψ in Fig. 2 is $\pi/2-\phi$; it has been computed from (2), entered in column 2 of Table I, and plotted in curve 1, Fig. 3. The values are accurate to one-half minute of arc.

To find the ray path and horizon distance, the angle δ between the tangent to the ray and the tangent to the earth at the earth-grazing point of the ray is computed using

$$d\delta/dz=-\tan\phi[d\mu/dz]/\mu, \tag{4}$$

TABLE I.

Altitude in Thousands of Feet	Dip of Horizon	Horizon Distance, Nautical Miles	Refraction, in Minutes
z	ψ	D	δ
0	0° 0′	0	0.00
2	43	52	8.71
4	1° 1	73	12.14
6	15	89	14.65
8	27	103	16.67
10	38	16	18.35
12	47	27	
14	56	37	
16	2° 05	46	
18	13	55	
20	20	63	24.06
22	28	72	
24	35	80	
26	41	87	
28	48	93	
30	54	200	
32	3° 00	07	
34	6	14	
36	11	20	
38	16	26	
40	22	31	
42	27	37	
44	32	42	
46	36	47	
48	41	52	
50	46	57	31.08
52	50	61	
54	55	66	
56	59	71	
58	4° 03	75	
60	07	80	
62	11	84	
64	15	88	
66	19	92	
68	23	96	
70	27	300	
72	31	04	
74	35	08	
76	39	12	
78	43	16	
80	47	20	
82	51	24	
84	55	28	
86	59	32	
88	5° 03	36	
90	06	39	
92	10	43	
94	14	47	
96	18	51	
98	22	55	
100	26	59	32.92

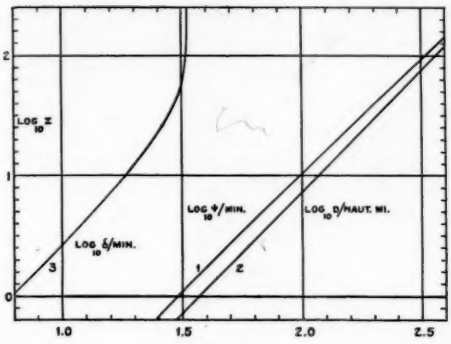

FIG. 3. Curves of dip, refraction and horizon distance.

gotten from (1) by putting $d\delta = d\phi$. Then the angle θ at the earth's center between the ray at height z and at height 0 is $\psi+\delta$; the horizon distance D is

$$D=(\psi+\delta)R.$$

The values of D and δ are entered in Table I and are plotted in Fig. 3.

To find the refraction of a ray of different index, we get from (3) and (4)

$$\frac{\partial}{\partial a}\left(\frac{d\delta}{dz}\right)=\frac{\partial}{\partial a}\left(-\frac{a(d\rho/dz)}{1+a\rho}\tan\phi\right)$$

$$=\frac{-1}{(1+a\rho)^2}\tan\phi\frac{d\rho}{dz}$$

$$-\frac{a}{1+a\rho}\frac{d\rho}{dz}\sec^3\phi\frac{R}{R+z}\frac{1-\rho}{(1+a\rho)^2}$$

$$=-\frac{d\rho}{dz}\frac{\tan\phi}{(1+a\rho)^2}\left[1+\frac{1-\rho}{\cos^2\rho}\cdot\frac{a}{1+a}\right],$$

using

$$\sin\phi=\frac{R}{R+z}\frac{1+a}{1+a\rho}.$$

Thus

$$\frac{\partial}{\partial a}\left(\frac{d\delta}{dz}\right)=\frac{1}{a}\frac{d\delta}{dz}\cdot\frac{1}{1+a\rho}\left[1+\left\{\frac{1-\rho}{\cos^2\phi}\frac{a}{1+a}\right\}\right].$$

The term in braces has its greatest value at $z=0$; here it is

$$-\frac{1}{2}\frac{1}{1/(R(d\rho/dz)\,|_{z=0})+a}\doteq 0.109.$$

Thus, within 11 percent

$$\frac{\partial}{\partial a}\frac{d\delta}{dz}=\frac{1}{a}\frac{d\delta}{dz};$$

that is

$$\delta(a)=\frac{a}{0.000277}\cdot\delta(0.000277)$$

within about 1 percent over the visible spectrum. For example, in Table I the total refraction from 10^5 ft. to sea level for $\lambda 5800$ is 32′.9; for $\lambda 4900$, $a=0.000279$, and the total refraction is 33′.2. Since the atmosphere above 10^5 ft. makes a relatively negligible contribution to the total refraction these values refer to the tangent ray passing outside of the atmosphere. They are in accord with the observed astronomical value for visible light of about 33′ to 37′, the difference being attributable to variance of the atmosphere from the U. S. Standard Atmosphere.

To find the dip for a different index of refraction,

$$\frac{\partial}{\partial a}\phi=\frac{\partial}{\partial a}\arcsin\frac{R}{R+z}\frac{1+a}{1+a\rho}$$

$$\frac{\partial}{\partial a}\phi=\frac{1}{\cos\varphi}\frac{R}{R+z}\frac{1-\rho}{(1+a\rho)^2}$$

$$=\frac{(1-\rho)}{(1+a)(1+a\rho)}\tan\phi$$

$$\doteq(1-\rho)\tan\phi,$$

whence $\partial\psi/\partial a\doteq-(1-\rho)\cos\psi$.

Above 50,000 feet

$$\rho=10^{(0.2180-0.2074z/10{,}000\text{ ft.})}$$

from which

$$\sin\phi=\frac{R}{R+z}\cdot\frac{1.000277}{1+0.000277\rho},$$

and hence the dip ψ, can be calculated. D is then $(\psi+33')R$.

Correlation of Optical Properties and Photoelectric Emission in Thin Films of Alkali Metals

HERBERT E. IVES AND H. B. BRIGGS
Bell Telephone Laboratories, New York, N. Y.

(Received May 27, 1938)

INTRODUCTION

IN a series of papers on the photoelectric emission from thin films of alkali metal on specular supports of other metals (e.g. platinum and silver) a theory of such emission has been developed, and given experimental support.[1] According to this theory, the photoelectric emission is directly proportional to the rate of energy absorption in the alkali metal film, as determined by its optical absorptive properties and the energy density produced in it by reflection of light from the supporting metal. Both of these factors are derivable from the optical constants of the metals involved. This theory has been shown to give an immediate explanation of the high ratio of emissions for light polarized with the electric vector parallel to the plane of incidence, designated hereafter by the symbol ||, and at right angles thereto, designated hereafter by the symbol ⊥. *The variation of the emission with wave-length* predicted by the theory has had to await the determination of the optical constants of the alkali metals. These are now available,[2] and give an opportunity to make this further test of the theory. Results in general accord with the theory have already been published for potassium.[3] In this paper new experimental data for the three metals, potassium, rubidium and cesium are presented, and are compared with the predictions of the theory, both in its simple form, and as extended to cover more accurately the conditions which are indicated by the experiments as actually existing.

COMPUTED VALUES OF EMISSION FOR INFINITELY THIN FILMS

For sufficiently thin films (less than 10^{-8} cm) the energy density above the underlying metal is not appreciably affected by the alkali metal, and the energy absorbed becomes simply that energy times the absorption of the alkali metal. For the case of a platinum-iridium base (which was used in these experiments), the photoelectric emission as computed is shown in Figs. 1 and 2, for sodium, potassium, rubidium and cesium, using the recently determined optical constants. Fig. 1 gives the emission for light vibrating in the plane of incidence (||) and Fig. 2 for light vibrating at right angles thereto (⊥). It will be seen that the theory predicts for the first case sharp maxima of emission, at wave-lengths 2100A, 3400A, 3950A and 4350A; these maxima corresponding in position with the crossing points of the curves representing the values of the optical constants N and K_0 against wave-length. The maximum is highest, and the curve is narrowest for sodium, becoming progressively lower and broader for the other alkali metals in order. The expected maximum for sodium, drawn from extrapolated values of the optical constants, lies in the extreme ultraviolet, beyond

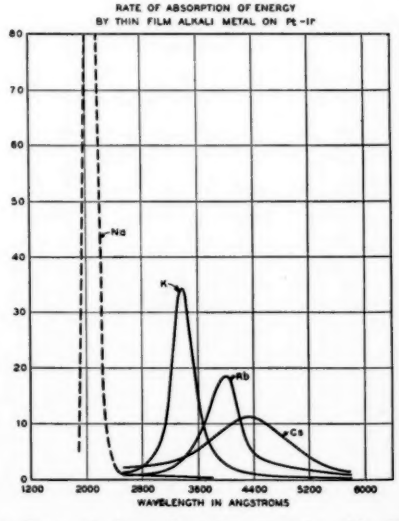

FIG. 1. Rate of absorption of energy by thin films of alkali metal on Pt-Ir; || light, film thickness 10^{-8} cm.

[1] Herbert E. Ives, Phys. Rev. **38**, 1209 (1931). Herbert E. Ives and H. B. Briggs, Phys. Rev. **38**, 1477 (1931); **40**, 802 (1932); J. O. S. A. **26**, 247 (1936).

[2] Herbert E. Ives and H. B. Briggs, J. O. S. A. **26**, 238 (1936); **27**, 181 (1937); **27**, 395 (1937).

[3] Herbert E. Ives and H. B. Briggs, J. O. S. A. **26**, 247 (1936).

the range of study with our apparatus, and accordingly our experiments have been confined to the three other alkali metals. In the case of light with the electric vector parallel to the surface ($\perp$) the predicted emissions show no well defined maxima and are, as the scales show, extremely small as compared with the $\parallel$ emissions.

Apparatus

The apparatus used in the present study has been rather completely described in earlier papers, so that attention need be given mainly to certain improvements which have been made. These improvements are chiefly in the design of the photoelectric cells, and in the method used to evaluate the monochromatic energy used in making the measurements.

In the cells the principal novelty is the development of a design which completely prevents leakage of current along the cell walls due to the formation on them of alkali metal films. These conducting films have always been a source of experimental trouble, which increases in seriousness with every improvement in the purity of the alkali metal and in the vacuum, and is so great with the lower melting point metals as to threaten to prevent all measurements with the low intensities of illumination obtainable from a monochromator. Previously we have experimented with guard rings and with heating coils around the necks of the tubes,

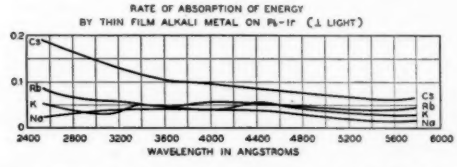

Fig. 2. Rate of absorption of energy by thin films of alkali metal on Pt-Ir; $\perp$ light, film thickness 10^{-8} cm.

but without entirely satisfactory results. In the tubes used in this investigation we have attacked the problem from a different angle, and with entire success. In place of local heating of the cell we have resorted to local cooling, in conjunction with a labyrinth structure, such that the deposition of metal from the vapor is complete in the cooled region, thus preventing the formation of conducting films over an extended section of the tube.

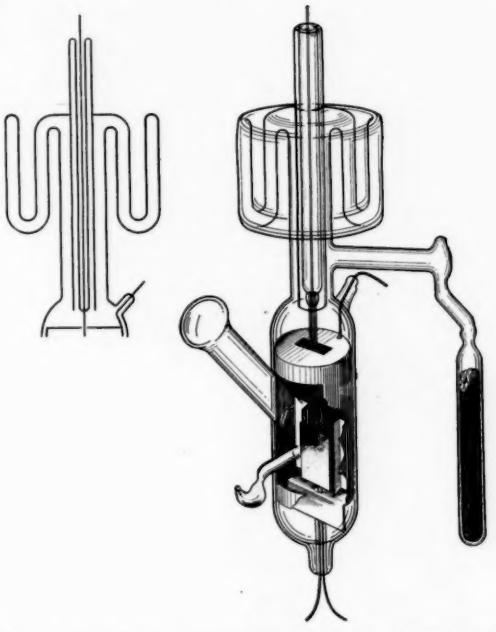

Fig. 3. Quartz windowed cell used for photoelectric investigation of the alkali metals.

The construction adopted is shown in Fig. 3. The labyrinth at the top, is, as shown, of such a form that liquid air may be poured into it, and maintained at such a level that the alkali metal atoms no matter how great their free path, must eventually strike and condense upon the glass without passing beyond the cooled region, thus leaving a considerable portion of the glass labyrinth between anode and cathode free of film. The cell walls, which absorb strongly photoelectrically sensitive layers, are connected with the cylindrical anode, so that they contribute no current. This method of avoiding leaks proved completely successful, permitting continuous observations over many hours. After allowing the liquid air to evaporate, the cells could be restored to working condition by immersing the lower part in liquid air and placing a furnace around the labyrinth until all alkali metal was trapped in the lower section. Fig. 4 shows a photograph of one of the cells.

In the measurement of the intensity of the radiation from the (double) monochromator, a quartz window cesium photoelectric cell was used, specially sensitized to give a broad spectral

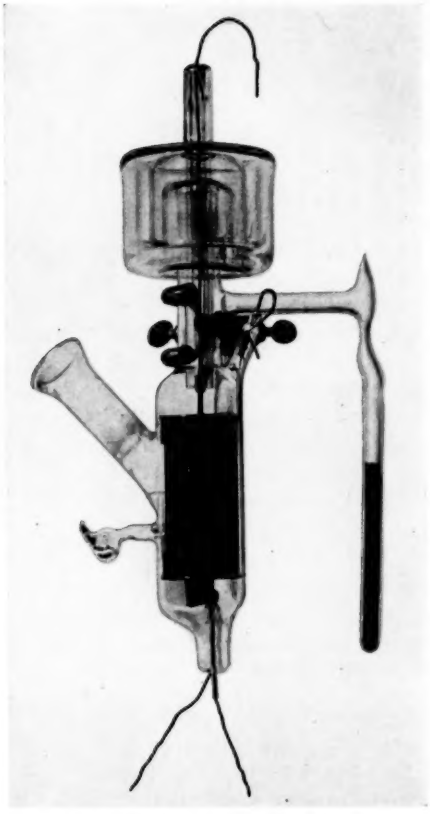

FIG. 4. Photograph of a finished tube.

response. This was calibrated as a separate experiment, against a vacuum linear thermopile.[4] This cell, mounted to one side, was illuminated by sliding in a 45° front surface aluminized mirror. A great advantage of using the photoelectric cell as an energy reference standard lay in its stability, and in the fact that the same indicating apparatus (electrometer) was used, after the calibrating operation, for all measurements. An important characteristic of the measurements so made is that they are all on the same scale, independent of variations between thermopile and test cell electrometer sensitivity. As a consequence, long series of measurements showing the history of film growth were obtainable which were reproducible at will and gave a confidence in the relative values of current at different stages which was previously not possible.

In the experiments to be described and discussed precision observations were confined to light vibrating in the plane of incidence (‖). This limitation of field of study was made in part because the crucial phenomena—the occurrence and position of the maxima of emission—are to be found for light so polarized. In addition the difficulties of securing accurate data for ⊥ light are very considerable, due to the very small values of the photoelectric currents, but chiefly because quite small and unavoidable admixtures of ‖ light due to scattering in the quartz windows and other optical parts are sufficient to mask and distort the results. Some observations by ⊥ light were made to give qualitative checks on the nature of the resultant emissions, and will be noted where significant, but unless otherwise noted the data and discussion apply entirely to ‖ light.

EXPERIMENTAL RESULTS

The experimental procedure used with each alkali metal was the same; as follows: The alkali metal, which had been multiply distilled into a small side tube, was driven by flaming into the main tube, which, as in all our work, was thoroughly outbaked, and allowed to diffuse freely, the cooled labyrinth keeping it off a section of the wall, as above described. The body of the tube was then immersed in liquid air and the platinum-iridium cathode raised to white heat by electron bombardment, thereby being rendered completely insensitive, after cooling, in the spectral region under study. The liquid-air flask was then lowered a little, so that some of the alkali metal trapped on the walls could give off vapor. The cathode thereby became sensitive, and measurements were made through the spectrum. The liquid-air flask was then lowered further, and measurements again made; the process being continued until finally the cell assumed room temperature. After standing for a time at room temperature a steady state was attained, corresponding to the formation of an *equilibrium film*, which would remain unaltered

[4] A surface thermopile if available would have been preferable, as the exact adjustment of the monochromator slit image on the linear element, especially with invisible radiation, presents difficulties which inevitably impair the accuracy of the resulting calibration.

and give identical measurements for as long as one wanted to maintain the insulating labyrinth.

The *growth history* of the film follows the same course for each metal, as shown in Figs. 5, 6 and 7. Referring to the results for rubidium (Fig. 6) which are the most detailed, we observe an initial appearance of sensitiveness in the extreme ultraviolet, which increases with film growth, the long wave limit continuously increasing, the emission being at all times progressively greater toward the shorter wave-lengths. At a certain point this growth toward long wave-lengths ceases, the ultraviolet emission begins to fall, and as the equilibrium condition is attained, a maximum of emission develops, which for rubidium is near wave-length 3800A.

Growth histories are shown in Fig. 5 for potassium and in Fig. 7 for cesium. Those for potassium are similar in general character to those for rubidium, just discussed. In the case of cesium there is a marked difference of behavior in that the equilibrium film is less sensitive at all wave-lengths than the films which immediately precede it, instead of surpassing those at its wave-length maximum as is the case with rubidium and potassium. This peculiarity was checked by many repetitions of the growth process, in two different tubes.

Of the process before the attainment of the equilibrium condition it need merely be said here that this is correlated with the reduction

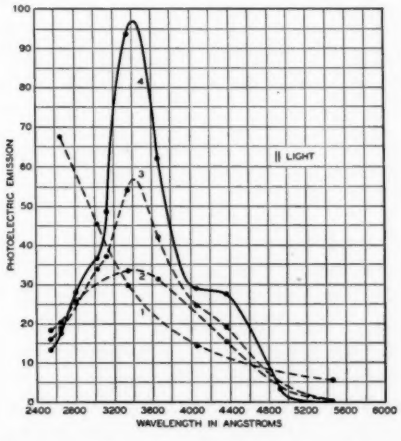

FIG. 5. Growth of sensitivity, K on Pt-Ir. Curves numbered in order of growth. Full line represents equilibrium film response.

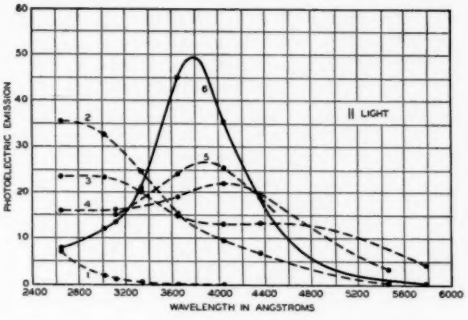

FIG. 6. Growth of sensitivity, Rb on Pt-Ir. Curves numbered in order of growth. Full line represents equilibrium film response.

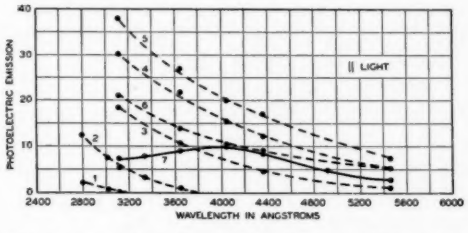

FIG. 7. Growth of sensitivity, Cs on Pt-Ir. Curves numbered in order of growth. Full line represents equilibrium film response.

of the work function of the platinum-iridium by isolated atoms or groups of atoms. The photoelectric emission is here related to the optical constants of the supporting metal, and not to those of the alkali metal, as shown by our earlier experiments on silver.[5]

We proceed at once to consider the equilibrium films. For this purpose we have plotted in Fig. 8 the equilibrium film emission data for all three metals, along with the computed values previously given in Fig. 1 for infinitely thin films. We note at once that we have the expected maxima, in the order as to position and relative magnitude indicated by the simple theory. We find however that the emission maxima are in general *broader*, and that their position is shifted, slightly toward the red in the case of potassium; in the case of rubidium and cesium, considerably and progressively toward the ultraviolet. Thus the predicted and observed maxima lie for potassium at 3400A and 3450A, respectively;

[5] Herbert E. Ives and H. B. Briggs, Phys. Rev. **40**, 802 (1932).

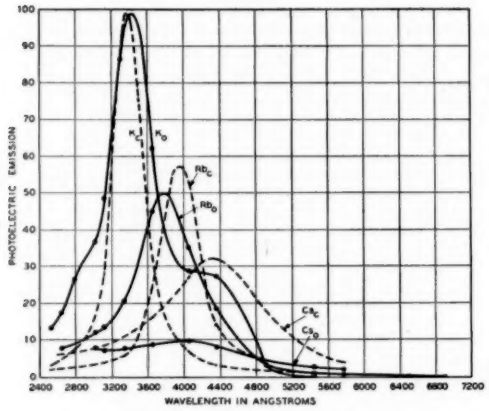

FIG. 8. Comparison of observed photoelectric emission (subscript *o*) for equilibrium film thickness, and calculated energy absorption (subscript *c*) for film thickness of 10^{-8} cm; || case, for K, Rb and Cs on Pt-Ir.

for rubidium at 3950A and 3800A respectively, and for cesium at 4350A and 4000A.

These discrepancies of shape and position have led us to a more detailed study and development of the underlying theory, to see if these results are explainable by it.

More Detailed Theory

In surveying the theory as simply applied in Fig. 1 we note the assumption that the alkali metal film has been considered so thin as to have no appreciable effect on the standing wave pattern set up above the platinum-iridium. This assumption was supported by earlier measurements on the optical properties of film-covered glass and platinum, and there was nothing in our previously reported or in the new photoelectric measurements on potassium films to indicate any substantial error in this assumption. It appears however necessary to investigate whether this assumption can be made in the case of rubidium and cesium. In order to investigate this question we have had computations made of the results to be expected with various thicknesses of alkali metal.

In these computations it is assumed that the emission of electrons occurs only from the topmost layer of the film, or, what amounts to the same thing, that only those electrons originating in the topmost layer can escape. We then, by the methods which have been published by Fry,[6] investigate the energy density in this layer, due to the reflection of light from a base consisting of platinum-iridium overlaid by various thicknesses of alkali metal.

The results of these computations for rubidium for both the || and ⊥ cases are shown in Fig. 9. We see that as the alkali metal film increases in thickness, the maximum of emission *decreases in magnitude, broadens, and shifts toward the shorter wave-lengths*, which are precisely the characteristics in which the computed curve differed from our experimental equilibrium curve for rubidium as shown in Fig. 8. Also as shown in the lower figure the ⊥ curves become higher relative to the ||, giving lower ratios of || to ⊥ than for the infinitely thin case. Similar considerations apply to cesium, and with modifications to be described later to potassium also.

A second factor which has also to be considered, is the ability of the photoelectrons to escape from the alkali metal after their release by light. The optical theory here developed has nothing to say with respect to this factor. It calls for the generation of photoelectrons at all wave-lengths, including the infra-red; it indicates no long wave threshold. In conformity with experiment there is needed in the theory

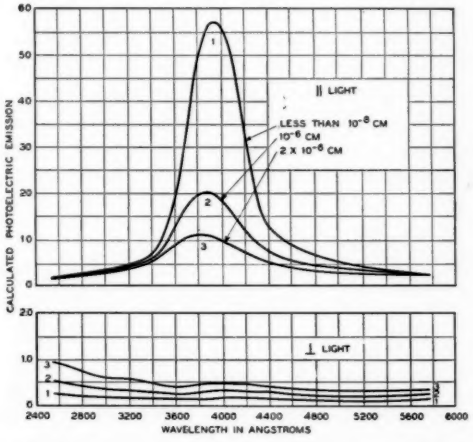

FIG. 9. Variation in rate of absorption of energy at the surface with increasing thickness of rubidium on Pt-Ir. Numbers of lower group correspond with those of upper group.

[6] Thornton C. Fry, J. O. S. A. and R. S. I. **15**, 137 (1927); **16**, 1 (1928); J. O. S. A. **22**, 307 (1932).

an additional function of frequency which shall be zero at the threshold and shall increase with frequency. It must represent the increased energy of emission $(h\nu - h\nu_0)$ with increase of frequency, and the consequent greater number of photoelectrons which are able to escape. Since part of this increased number escaping are contributed from greater depths, the complete expression for this additional function will include some modification of the assumption made as to the depth from which the photoelectrons are emitted.

Our information on the conditions necessary for the escape of the photoelectrons is insufficient to yield the exact form of this additional factor, but a reasonable assumption would be that it is a linear multiplying factor, of the form $\nu - \nu_0$, which satisfies the condition that the energy effective for releasing photoelectrons is zero at the threshold and beyond, and increases linearly with the frequency. The result of such a factor would be in general to tilt the computed curves about the photoelectric threshold as a pivot, with little effect on the position of sharp maxima.

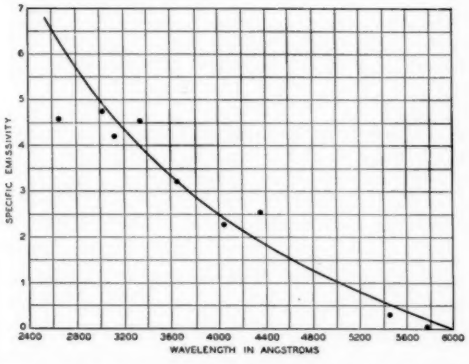

FIG. 10. Full curve represents $\nu - \nu_0$ plotted against wave-length for long wave limit of 6000A. Points give specific emissivity for rubidium, || case.

We have plotted this emission function, which we may call the *specific emissivity*, for each of the alkali metals, using the appropriate threshold frequency as determined by experiment in Figs. 10, 12, 14. On the wave-length scale, which is used in conformity with the other figures, the function shows a slight curvature (due to the reciprocal relation between frequency and wave-length). The plotted points are obtained by

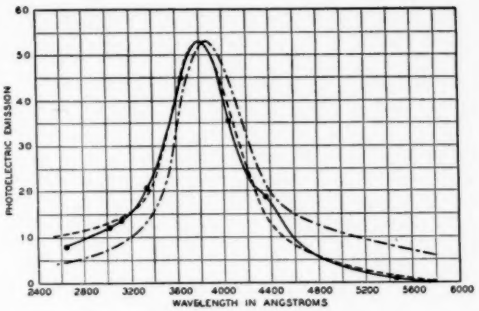

FIG. 11. Comparison of computed and observed emissions for rubidium on Pt-Ir, || case. Full line is photoelectric emission for equilibrium film; dash and dot is energy absorption for film 10^{-6} cm thick; dashed curve is the energy absorption modified by the $\nu - \nu_0$ factor.

dividing the experimental values by the calculated, using for the calculated that thickness which gives the best fit for the *breadth* of the experimental maximum. The relation of the points to the curves is fairly good for rubidium and cesium, the wide divergence for potassium in the blue will be discussed later.

Using the two further developments of the theory, as just described, we can now investigate whether we can take up the discrepancies which appeared in the application of the simple theory in Fig. 8. We shall consider first our data for rubidium. Referring to Fig. 11 we have the experimentally determined emission shown by the full circles and the full line. The dot and dash line shows the absorption of the surface layer for a film 10^{-6} cm thick. It has closely the breadth of the experimental curve, but is shifted to the red, is too high on the red side, and does not diminish to the experimental threshold, at 6000A. The dashed curve is the absorption curve just described after applying the $\nu - \nu_0$ correction and a change of scale to match the magnitude of the experimental curve at its maximum. The agreement with the experimental data is, it will be seen, quite close, and we believe warrants the assertion that the theory is well verified.

In Fig. 13 are shown the results of similar computations for cesium. The full curve as before joins the experimentally determined points. The dashed curve is that computed for a thickness of 8×10^{-7} cm. It is quite broad and flat compared with the infinitely thin film curve

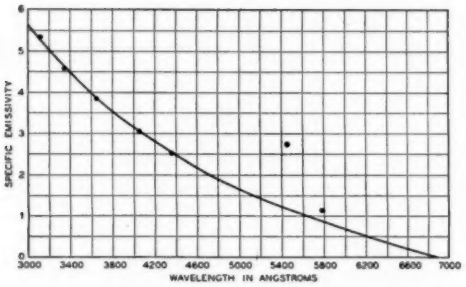

FIG. 12. Full curve represents $\nu-\nu_0$ plotted against wave-length for long wave limit of 6900A. Points give specific emissivity for cesium on Pt-Ir, || case.

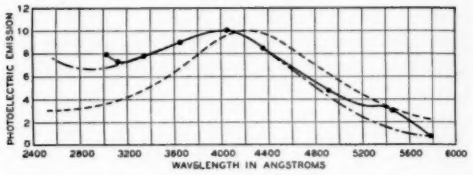

FIG. 13. Comparison of computed and observed emissions for cesium on Pt-Ir, || case. Full line is photoelectric emission for equilibrium film; dashed curve is energy absorption for film 8×10^{-7} cm thick; dash and dot same after applying $\nu-\nu_0$ correction.

of Fig. 1, while nearly matching the experimental curve in breadth it does not decline to a zero threshold, and is tilted upward on the red side. The dot and dash curve, the result of applying the $\nu-\nu_0$ factor gives a reasonable match with the experimentally determined curve. We observe on the red side, as with rubidium (Fig. 11) indications of a secondary maximum on the red side. This is possibly of the same nature as the very marked secondary maximum occurring with potassium, which will be discussed at some length.

Turning now to the results for potassium we find a more complicated problem. The experimental data actually fall so close to the computed values for an "infinitely" thin film, as to have led us to interpret them as confirmatory of the simple theory.[3] It develops however that upon using the thickness necessary to match the breadth of the curve, and upon introducing the specific emissivity factor, the desired agreement between experiment and theory can be obtained only by assuming somewhat different optical constants for potassium. In detail, we note first from Fig. 8, that the computed emission for a film of $<10^{-8}$ cm, shown by the dashed line, lies slightly to the short wave side of the experimental data (full line curve), instead of the long wave side as with rubidium and cesium. We note further that the problem of finding a thickness for which the computed curve has the same breadth as the observed is complicated by the presence of a secondary maximum or step at 4400A, whose extent and influence on the breadth of the whole emission curve is problematic

In our earlier paper on our first results on potassium alone[3] we have pointed out that this secondary maximum, which is almost certainly due to the presence of hydride, varies in size from cell to cell, and that concurrently the position of the principal maximum of the emission curve shifts, being moved further toward the red the more pronounced the secondary maximum. This shift can hardly be a summation of the potassium and potassium hydride emission curves, since the latter will be low and flat where the former has its maximum. It is far more probable that the presence of the hydride causes a change in the optical properties of the potassium, shifting the crossing point of the N and K_0 curves toward the red.

Following this assumption we have first arrived at a thickness (7×10^{-7} cm) which gives a good match for breadth with the experimental curve. This is shown as the dotted curve of Fig. 15. The divergence between the maxima for the calculated and observed values amounts to about 140A. We have accordingly assumed for purposes of computation, a set of potassium optical constants shifted toward the red by 140A. (This shift is actually very small in terms of the experimental uncertainties of the optical constant determinations, the values fall well inside the spread of the published experimental curves.) Using the modified values of the optical constants we have calculated the emission curve for a thickness of 7×10^{-7} cm, and have applied to this the $\nu-\nu_0$ factor, as previously described. The resultant curve, shown by the dot and dash line in Fig. 15, gives a satisfactory agreement with the experimental curve, except on the red side, where the secondary (hydride) peak occurs. Finally we have subtracted the computed (dot and dash) curve from the experi-

mental, giving the points indicated by circles. Through these we have traced (dotted line) an experimentally determined potassium hydride emission curve. The agreement of this latter curve with the points obtained by subtraction confirms the hypothesis that this secondary maximum is indeed due to the presence of hydride. Reversing the procedure, that is, subtracting the hydride curve from the experimentally found emission, leaves us with a very

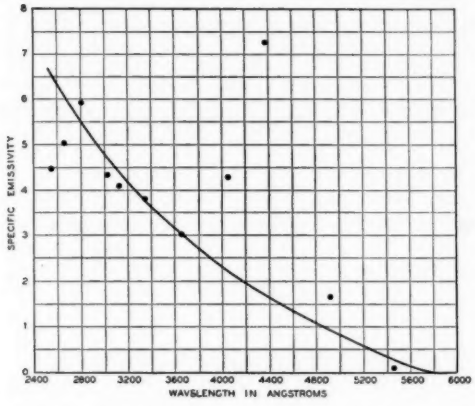

FIG. 14. Full curve represents $\nu-\nu_0$ plotted against wave-length for long wave limit of 5800A. Points give specific emissivity for potassium on Pt-Ir, || case.

close agreement between the observed emission curve and that computed for a thickness of 7×10^{-7} cm, using the slightly altered optical constants, justification for which has been given above.

The experimental data and computations which have just been given complete the main problem of this investigation, which is the correlation of the optical properties and photoelectric emission for the case of light polarized with the electric vector in the plane of incidence (||). As already stated conditions for observations with $\perp$ light were unfavorable, nevertheless it may be recorded that sufficient observations were obtained to verify the chief prediction of the theory, which are (1) that the spectral maxima of emission characteristic of the || case are absent, (2) that the emission for $\perp$ light is quite small compared with that for || light, usually being only a few percent of the latter, (3) that the emission is, after making reasonable allowance for admixtures of || light, of the order of magnitude in comparison to the || emission corresponding to the thicknesses deduced from the || emissions.

DISCUSSION

The principal contribution of this investigation to the theory of thin film photoelectric emission is the postulation of rather considerable film thicknesses in place of the monatomic films (10^{-8} cm or less) which have been rather generally assumed heretofore.

The film thicknesses used in the calculations were chosen to give the best fit between the calculated and observed emissions. For potassium this thickness was 7×10^{-7} cm, for rubidium 10^{-6} cm and for cesium 8×10^{-7} cm. In terms of atomic diameters,[7] these thicknesses would be respectively 15, 20 and 15. The above estimates are of course only approximate, as they depend on the choice of the function to represent intrinsic emissivity. However, the evidence from the experiments appears to us quite strong that the films must have thicknesses of this order of magnitude. We know of no compelling reason to believe that the attractive forces of the platinum-iridium base are completely satisfied by the first layer of adsorbed atoms. There is

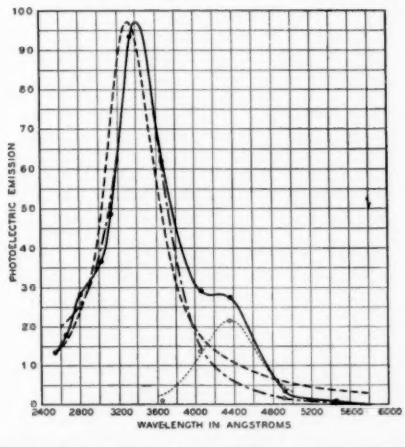

FIG. 15. Comparison of computed and observed emissions for potassium on Pt-Ir, || case. Full curve is photoelectric emission for equilibrium film; dashed curve is energy absorption for film 7×10^{-7} cm thick; dash and dot same after shifting 140A and applying $\nu-\nu_0$ correction.

[7] F. Laves, Naturwiss. **25**, 731 (1937).

also no compelling reason to believe that the films go down in perfectly uniform layers. If they built up uniformly by atomic increments we would expect to observe the high relatively sharp maxima predicted for very thin films (Fig. 1) as a stage in the growth history, preceding the equilibrium film. Since this does not occur we are forced to the conclusion that patches start to build up in thickness before the surface is completely covered. Microscopic examination of the cesium equilibrium films in fact frequently shows the metal to have deposited in small globules, in agreement with the idea that the films can increase in thickness locally before the whole surface is covered.

Summary

In this paper we have described an experimental investigation undertaken to test a theory which correlates the photoelectric emission of thin films of alkali metals with the optical properties of the alkali metals and the base on which they are deposited. The theory is built on the simple assumption that photoelectric emission is proportional to the rate of absorption of energy in the topmost layer of the alkali metal film. We have found the theory as developed on the original assumptions to give approximate agreement with experiment, and have then extended the theory by introducing reasonable additional factors. The extended theory gives a close agreement with the experimental findings. The characteristic phenomena, namely the maxima of emission occurring in the spectral response curves of photoelectric emission, appearing only for light polarized in one plane, are qualitatively and quantitatively explained in terms of the optical constants.

A Further Search for the Ideal Color System

II. A Reconsideration of the Helmholtz Line Element

R. H. SINDEN
Wolcott, New York

(Received June 14, 1938)

The first paper of this series proposed a re-examination of the Helmholtz colorimetric line element, and described a new mechanico-graphical device that has been employed to assist in selecting the coordinate system for which this expression gives best agreement with modern colorimetric data. The coordinate system thus found is fundamentally different from the one determined by Helmholtz himself, and brings about a greatly improved agreement with experimental measurements. In the present paper the new coordinate system is defined, and numerical results afforded by the Helmholtzian function within this frame of reference are compared with observed data and also with the consequences of another theoretical construction. Conclusions are reached concerning the tenability of the assumptions upon which Helmholtz' derivation rests.

I. The Optimum Coordinate System

THE general and special forms of the Helmholtz colorimetric line element (Eqs. (H-1) and (H-2) of the preceding paper of this series[1]) may be written:

$$KdE=[\Sigma(d\log x_i)^2]^{\frac{1}{2}} \quad (i=1, 2, 3) \qquad (1)$$

and

$$KdE=[\Sigma(du_i)^2]^{\frac{1}{2}}, \qquad (2)$$

where $u_i=\log x_i/x_{i+1}$ $\quad (x_4=x_1)$.

The second of these is applicable to the experimental case where equality-of-brightness conditions prevail, and leads to the equation

$$K\Delta E=[\Sigma(\Delta u_i)^2]^{\frac{1}{2}} \quad (\Delta u_i=u_i'-u_i), \qquad (2A)$$

in which ΔE (with suitable choice of the unit-fixing constant, K) is the least number of unit chromaticity steps between two colors C and C' whose coordinates in the color space are, respectively, x_1, x_2, x_3 and x_1', x_2', x_3'.

The x_i of these expressions are connected with coordinates y_k in any other color system by the transformation

$$x_i=\Sigma_k a_{ik}y_k \quad (k=1, 2, 3). \qquad (3)$$

The initially unknown coefficients of Eqs. (3) have been determined upon the principle of best agreement with experimental data, by the method described previously,[1] and are given below with respect to the reference system of the "1931 I.C.I. Standard Observer"[2] whose color coordinates are designated by x, y, z. Luminosity coefficients, L_i, based on the standard I.C.I. luminosity data are also given.

$$\left.\begin{aligned} x_1&=0.637x+0.262y-0.0885z \\ x_2&=-0.335x+1.071y+0.0852z \\ x_3&=0.373x+0.1456y+0.373z \end{aligned}\right\}, \qquad (3A)$$
$$L_1=1.000, \quad L_2=1.726, \quad L_3=-0.1571.$$

The locus of spectrum colors on the plane $\Sigma x_i=1$ in the color space defined by Eqs. (3A) is shown in Fig. 1 by the solid curve. The points R, G, B represent, respectively, the three spectral cardinal stimuli of the I.C.I. system ($\lambda\lambda$700.0, 546.1, 435.8 mμ). The point W at the center of the x_i triangle represents the color evoked by a stimulus of 4800°K Planckian distribution as seen by an observer with "normal" retinal pigmentation (i.e., the amount of pigmentation assigned to the I.C.I. Standard Observer). This particular "standard white" had been adopted chiefly for the sake of convenience in effecting a comparison of the theoretical construction with certain experimental data.

II. Derivation of Theoretical Chromaticity Sensibility Functions

Numerical results afforded by Eqs. (2) and (2A) in the color space defined by Eqs. (3A) are graphically compared with experimental chro-

[1] R. H. Sinden, J. O. S. A. **27**, 124 (1937).

[2] D. B. Judd, "The 1931 Standard Observer and Coordinate System for Colorimetry," J. O. S. A. **23**, 359 (1933).

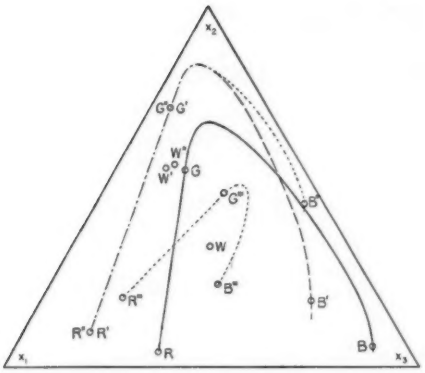

FIG. 1. Trilinear diagram on the plane $\Sigma x_i = 1$, showing various color charts. *RGBW*, from Eqs. (3A); *R'G'B'W'*, from Eqs. (3A) with change of units; *R''G''B''W''*, from Judd uniform-chromaticity-scale triangle (displaced); *R'''G'''B'''W'''*, from Helmholtz color triangle.

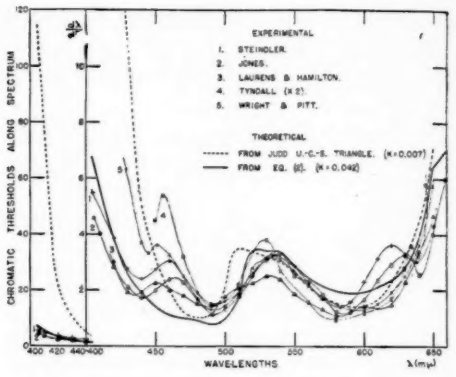

FIG. 2. Wave-length change thresholds along the colorimetrically pure spectrum.

maticity sensibility measurements of various species in Figs. 2 to 6. Fig. 2 compares observed and computed widths of unit chromaticity steps (i.e., least perceptible differences of chromaticity) along the objectively pure spectrum. Replacing its differentials by derivatives with respect to λ and inverting, Eq. (2) gives

$$d\lambda/dE = K[\Sigma(du_i/d\lambda)^2]^{-\frac{1}{2}}.$$

The derivatives in this expression may be readily evaluated graphically by constructing tangents to the curves for the u_i plotted against λ.

Figure 3 shows purity-step counts from "white" to spectrum colors. The computed values of ${}_W(\Delta E)_H$ are for the intervals between the point *W* in Fig. 1 and points on spectral locus *RGB*. Since at the point *W*, $u_1 = u_2 = u_3 = 0$, Eq. (2A) becomes

$${}_W(\Delta E)_H = 1/K[\Sigma(u_i)_H^2]^{\frac{1}{2}}.$$

Figures 4, 5 and 6 represent chromaticity-step widths at interior points in the Newtonian color chart. These three graphs have been reproduced directly from illustrations in the treatise by Judd[3] to which frequent reference is made further on, its author having very kindly not only granted the writer permission to do so, but also furnished him with some excellent prints from which cuts could be made. The painstakingly plotted experimental points and the corresponding curves derived from Judd's "uniform-chromaticity-scale triangle" belong to the original figures; curves derived from Eq. (2) have been added.

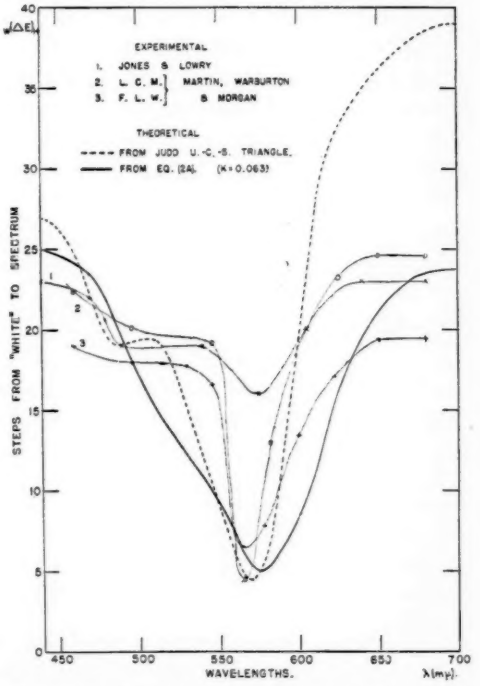

FIG. 3. Numbers of purity-change steps along lines on the color chart connecting the point *W* (locus of 4800°K Planckian) and points on the spectral locus designated on the wave-length scale.

The experimental data shown are stated in terms of dominant wave-length and colorimetric

[3] D. B. Judd, "A Maxwell Triangle Yielding Uniform Chromaticity Scales," J. O. S. A. **25**, 24 (1935).

purity. The colorimetric purity, p_c, of a given color, C, is defined as $L_H/(L_H+L_W)$, where L_H and L_W are the luminosities respectively of the spectral and standard white components in a chromatically equivalent mixture. The corresponding data due to Eq. (2) must be obtained graphically, and the simplest method to accomplish this is to project the color chart upon a plane of uniform brightness[4] in the x_i space. In so doing, the units in which the x_i are measured may be altered so as to give an equilateral triangular coordinate network on the resulting diagram, thus simplifying the construction. On the uniform-brightness diagram, a portion of which is illustrated in Fig. 7, if a straight line is drawn from the white point, W, so as to pass through the point C and cut the spectral locus at H, then $p_c=d/D$, where d is the distance WC, D the distance WH; so that distances on the diagram may be readily translated into terms of colorimetric purity, and *vice versa*.

The experimental data represented in Fig. 4 were got by altering the proportions of the constituents in mixtures of a spectral color and a standard white until just perceptible differences of chromaticity were set up. To obtain comparable data based on Eq. (2), radial lines were drawn from the point W on the uniform-brightness diagram, cutting the spectral locus at stated points on the wave-length scale. The theoretical chromatic threshold in the neighborhood of some point C on one of these lines is given by

$$\Delta p/\Delta E = K[\Sigma(\Delta u_i)^2]^{-\frac{1}{2}}(\Delta d)_c/D,$$

in which $(\Delta d)_c$ is a short segment laid off along the line with C as its center. The length $(\Delta d)_c$ may be taken equivalent to one unit chromaticity step, so that $K[\Sigma(\Delta u_i)^2]^{-\frac{1}{2}}=1$, when more simply

$$\Delta p/\Delta E = (\Delta d)_c/D.$$

The experimental data of Fig. 5 were obtained by varying the wave-length of the spectral component in mixtures of the above type, keeping the luminosity ratio of the two components constant, until a difference in chromaticity became just perceptible. Similar data were derived from the uniform-brightness diagram in the following manner. Centering about points along radial lines like those already described, small ovoid closed curves were drawn, the

[4] Or brilliance. The recent preliminary report on nomenclature and definitions of the O. S. A. Committee on Colorimetry defines these two terms as synonymous and gives "brightness" preference. J. O. S. A. 27, 207 (1937).

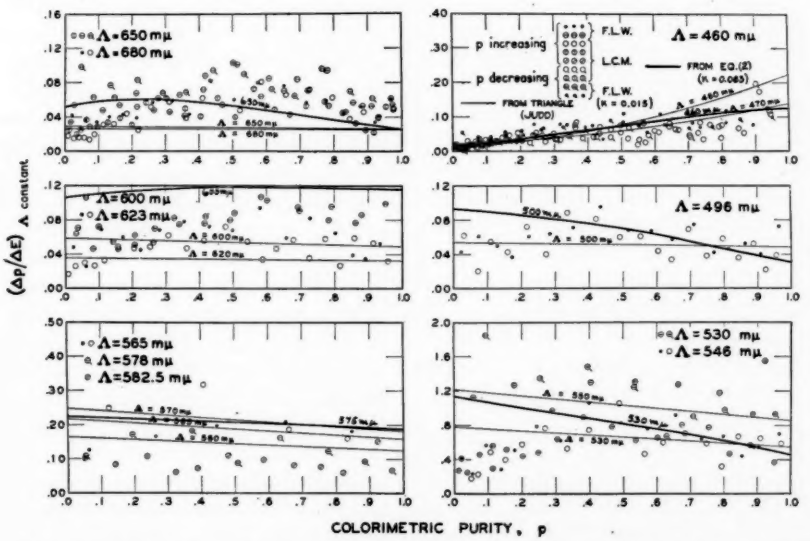

FIG. 4. (Taken from paper by Judd; curves derived from Eq. (2) added.) Purity-change thresholds at different purity levels along lines on the color chart connecting the point W and designated points on the spectral locus.

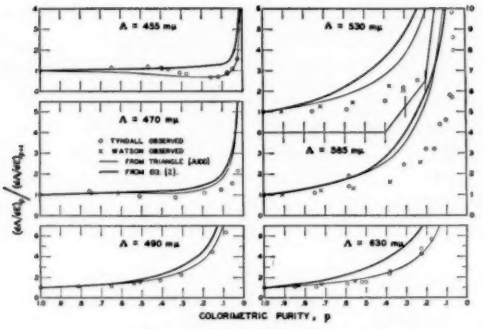

FIG. 5. (Taken from paper by Judd; curves derived from Eq. (2) added.) Dominant wave-length change thresholds (relative) at different purity levels along lines on the color chart connecting the point W and designated points on the spectral locus.

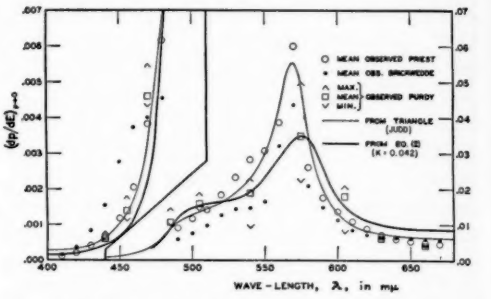

FIG. 6. (Taken from paper by Judd; curves derived from Eq. (2) added.) Purity-change thresholds at the point W on the color chart in directions indicated on the wave-length scale.

radii of which were determined by the relation $K^2\Sigma(\Delta u_i)^2=1$; so that, hypothetically, all points on the peripheries of these ovoid figures were one unit chromaticity-step removed from the central points. One such oval is shown in Fig. 7, centering about the point C on line WH. Other radial lines were now drawn in pairs, similar to lines WH' and WH'' in Fig. 7, each line so placed that its intersection with one of the ovals divided its length from W to the point where it cut the spectral locus in the same ratio as that in which the radial line passing through the center of the oval was divided by the latter point. Thus the points of intersection C' and C'' divide lines WH' and WH'', respectively, in the ratio WC/CH, so that $WC : WC' : WC''=WH : WH' : WH''$. The point at which a given one of the auxiliary radial lines cut the spectral locus then indicated the extent of the shift in wave-length of the spectral component hypothetically necessary to produce a just perceptible difference in chromaticity in a mixture originally of color C under the stated experimental conditions; and if $(\Delta\lambda)_{p=1}$ is this shift when the points C and H coincide, $(\Delta\lambda)_p$ when the point C is in a position along the line WH specified by purity p, we have

$$(d\lambda/dE)_p/(d\lambda/dE)_{p=1}=(\Delta\lambda)_p/(\Delta\lambda)_{p=1}$$

to a first approximation. The plotted value of $(\Delta\lambda)_p/(\Delta\lambda)_{p=1}$ is in each case the mean of the two values measured in the directions of λ increasing and λ decreasing.

In Fig. 6 the curve due to Eq. (2) is plotted from data already used in Fig. 4, together with several additional points near the short wave end of the spectrum.

III. Comparison with Observed Data and Judd's Uniform-Chromaticity-Scale Triangle

Not all the available chromaticity-sensibility measurements have been utilized for the comparison, but those shown give a fairly adequate coverage of those portions of the color chart so far experimentally explored. The color-temperature series has been omitted, since the Planckian locus follows about the same course as some of the mixture series considered, and the agreement with experimental data along it is about the same. Judd,[5] who employed substantially the same data groups in establishing his uniform-chromaticity-scale triangle, has already fully discussed the qualifications of these data with respect to their present use, and little need be said here on that score.

The demonstrated close conformity of the "circle construction"[3] to experiment over much of the color chart area on Judd's uniform-chromaticity-scale triangle demands that a comparison be made with the results afforded by this construction, which, although empirically evolved, is entitled by virtue of its continuity throughout the color-chart area to be thought of as having a theoretical significance, and in fact would derive from a chromaticity distribution on

[5] See reference 3, also Deane B. Judd, J. O. S. A. **22**, 72 (1932).

planes of uniform brightness given by

$$KdE = [\Sigma(dx_i)^2]^{\frac{1}{2}}. \qquad (4)$$

A comparison with results afforded by Judd's "circle construction" is thus equivalent to a comparison with a theoretical color-space structure based on Eq. (4), and will be so regarded in the succeeding paragraphs. To facilitate such comparison, besides the curves in Figs. 4 to 6 contributed by the original figures in Judd's paper from which these are reproduced, curves derived from Judd's uniform-chromaticity-scale triangle have also been included in Figs. 2 and 3. The data for these latter curves were obtained by scaling similar graphs given in Judd's paper, with supplemental calculations by means of Judd's Eq. (4) for the region beyond λ440 mμ in Fig. 2.

In the interior regions of the color chart covered by Figs. 4, 5 and 6, there does not appear to be much choice as between Eqs. (2) and (4). In Fig. 4, Eq. (2) appears to follow the trend of the observed points somewhat more closely, especially for dominant wave-lengths near the extremes of the spectrum; while in Fig. 5, Eq. (4) lies a trifle nearer the experimental points in most cases. In Fig. 6, Eq. (4) is perhaps a little more representative of the mean of the experimental results, but the agreement of Eq. (2) with Purdy's data is very close indeed.[6]

Among the experimental curves in Fig. 3, although similar in general contour, there is considerable divergence as to the depth of the minimum. The two theoretical curves resemble the curves of Martin *et al.*[7] rather than that of Jones and Lowry[8] in this regard. The pronounced shoulder present on the short-wave side of the depression in all the experimental curves is lacking as a consequence of Eq. (2). Eq. (4) reproduces the shoulder in some degree but fails to preserve a proper balance between the heights of the two terminal regions.

In Fig. 2 a close similarity between the two theoretical curves is again to be noted over most of the range of the spectrum. In both, the positions and relative heights of the major maximum and minima agree fairly well with the aggregate of the experimental data. Judd has already discussed the absence of secondary minima in the curve corresponding to Eq. (4), pointing out that the experimental curve representing the combined data of five observers tested by Wright and Pitt[9] has no secondary minimum in the red and only a very slight one in the blue, and that in the earlier experimental determinations, where the use of filters for examining the terminal regions of the spectrum was omitted, the secondary minima may have been accentuated by the presence of stray light, which has that effect. Eq. (2) likewise gives no secondary minimum in the red and not more than a suggestion of one in the blue.

Laurens and Hamilton[10] conducted an extended series of measurements on chromaticity sensibility along the spectrum, enabling them to study the variations in the results of different individuals and also in those obtained from time

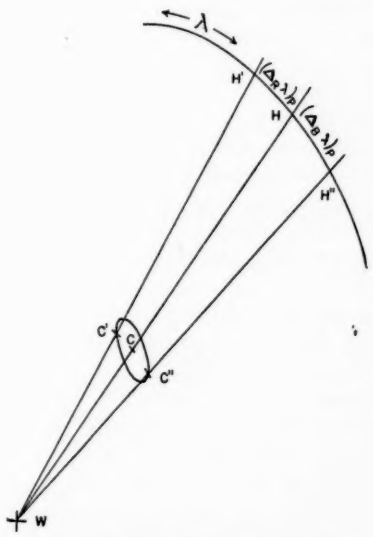

FIG. 7. Illustrative of the graphical construction employed on the uniform-brightness color chart.

[6] Cf. Judd, reference 3, for sources of experimental data plotted in Figs. 4 to 6.

[7] L. C. Martin, F. L. Warburton and W. J. Morgan, "Determination of the Sensitiveness of the Eye to Differences in the Saturation of Colours," Medical Research Council, Reports of the Committee upon the Physiology of Vision, XIII, Special Report Series, No. 188, London, 1933.

[8] L. A. Jones and E. M. Lowry, "Retinal Sensibility to Saturation Differences," J. O. S. A. and R. S. I. **13**, 25 (1926).

[9] W. D. Wright and F. H. G. Pitt, "Hue-Discrimination in Normal Colour-Vision," Proc. Phys. Soc. **46**, 459 (1934).

[10] H. Laurens and W. F. Hamilton, "The Sensibility of the Eye to Differences in Wave Length," Am. J. Physiol. **65**, 547 (1923).

to time by the same observer. In successive determinations by the same observer it was found that besides differences in the value of the chromatic threshold at any given point in the spectrum, there also occur slight lateral shifts of the positions of the maxima and minima. Consequently, if the arithmetic mean of several sets of observations is taken, the result is a flattened curve that fails to express the true course of any actual series of observations. The same holds true where the results of several different observers are concerned. The theoretical curves of Fig. 2 represent the averaged results of 17 individuals (upon whose combined data the standard I.C.I. color coordinates are based) and of a much larger number of separate series of observations; hence in view of the findings of Laurens and Hamilton it is hardly to be expected much trace would remain in them of the minor inflections present in the similar curves of individuals or small groups of observers.

Below about λ440 mμ in Fig. 2, the Eq. (4) curve rises much more steeply than the Eq. (2), as is brought out by the reduced-scale graph at the left-hand side of Fig. 2, and it is here that the best opportunity for a decisive test as between the two theoretical constructions appears to present itself. Unfortunately, reliable experimental measurements are all but lacking in this region, but those available do not indicate a sudden increase in $d\lambda/dE$ beyond λ440 mμ. In the interval between λλ440 and 405 mμ Jones[11] found 14 distinct chromaticity steps. Eq. (2) allows 11, Eq. (4) only 3. Steindler's[12] data, although of questionable dependability, confirm those of Jones.

The more recent determinations have not been carried to the far end of the spectrum, due, no doubt, to technical difficulties introduced by the low intrinsic luminosities of the spectral blues and violets. There may also be a tendency on the part of experimentalists to minimize the colorimetric importance of the region beyond about λ440 mμ because of that circumstance. Actually the low luminosity of this region in the spectrum of sunlight is fully offset, colorimetrically speaking, by its high neutralizing power. For example, from the data of the "I.C.I. Standard Observer" it may be found that complementary amounts of λλ405 and 571 mμ with standard illuminant "*B*" (approximating sunlight distribution) as "white," have relative luminosities 1 and 219, while the ratio of the ordinates corresponding to these wave-lengths in the standard luminosity curve for average noon sunlight (Abbott) is as 1 to 202. That is to say, a band of wave-lengths at λ405 mμ has a slightly greater influence than an equal band at λ571 mμ in determining the resultant chromaticity of undispersed sunlight. Additional chromaticity-sensibility data for the territory adjoining the extreme spectral violet are much needed, and should include not only measurements along the spectrum but also along the mixture series between "white" and violet, and the extreme spectral red and violet.

In order to bring the computed curve in each of the graphs of Figs. 2, 3, 4, and 6 to about the same average level as the observed curves or points, the constant K occurring in Eq. (2) and the equations derived therefrom has been assigned the two different arbitrary values indicated on the graphs. The value of K has been allowed to remain constant, of course, for any one group of observed data. Using different values for K in connection with the different data groups is justified on the grounds that the latter are taken from several separate sources, hence are subject to relative variations in measured threshold values arising from differences in experimental conditions and technique, to which measurements of this type are especially sensitive, and also from differences in individual observer characteristics.[3] The two values of K used differ in the ratio 1 : 1.5. To give agreement with the same data groups, Judd's "circle construction" requires values of K differing in the ratio 1 : 2.1; thus a somewhat wider range of variation of K is required by the latter than by Eq. (2) to give best agreement with the separate data groups, and if a single intermediate value of K is used, Eq. (2) gives a proportionately better representation of the entire body of data taken as a whole.

It is apparent that at no point do the consequences of Eq. (2) depart widely from the experimental data with which they have been compared. Yet the agreement is apparently not

[11] L. A. Jones, J. O. S. A. **1**, 63 (1917).
[12] Steindler, Sitzungb. d. Wiener Akad. **115**, 39 (1906).

everywhere within the tolerance limits set up by variations in the experimental results. The amount of data at present available is still too small for these tolerances to be very definite, except perhaps in the case of $d\lambda/dE$ (Fig. 2). Here the values given by Eq. (2) seem definitely somewhat too high from about λλ550 to 600 mμ and too low from about λλ450 to 500 mμ. In Fig. 3 a disparity exceeding experimental uncertainty between λλ500 and 550 mμ is also indicated.

IV. Interrelationship of the Theoretical Color Systems

The striking similarity on the whole of the two sets of theoretical curves strongly suggests that the two theoretical color systems from which they derive, although superficially appearing to be entirely distinct, are somehow interrelated; and the nature of the connection will now be investigated. In Judd's "circle construction" all loci of colors one unit chromaticity step removed from some given color are circles of equal radius. In the construction resulting from Eq. (2) such loci are approximately circular near the center of the diagram of Fig. 1, but depart from the circular more and more as the periphery is approached, with accompanying shrinkage in enclosed area:[13] thus the latter construction is nearest like the former at the center of Fig. 1, and least like it near the edges.

Color chart $RGBW$ in Fig. 1 is considerably off center with respect to the x_i triangle, but, since Eq. (2) is independent of units for the x_i, a change of units may be made that brings it to position $R'G'B'W'$ where it is roughly concentric with it and therefore embraces that part of its area in which the construction differs least from the uniform-chromaticity-scale diagram. Judd has pointed out in effect that the agreement of the latter with experimental data involves only the configuration of the color chart and not at all the choice of primaries, which is entirely arbitrary. In Fig. 1 Judd's color chart, defined by the four points R'', G'', B'', W'', is shown superposed upon chart $R'G'B'W'$ in such a manner that points R'' and G'' on the one coincide with points R' and G' on the other.

[13] Figure 2 of the preceding paper of this series, see reference 1.

The affinity of the two color systems now becomes self-evident. Near the center of the diagram they are almost identical, accounting for the close resemblance of the two sets of derived curves over this area. It is only near the end of the short wave limb of the spectral locus that a wide departure occurs, and it is also here that the derived curves conspicuously fail to agree.

That these two theoretical constructions are capable of representing so large a body of experimental facts with the fidelity with which they do obviously cannot be attributed to accidental circumstances. The inference that the one is theoretically correct, the other an approximation to it, must probably give place, however, for reasons presently to be enumerated, to the view that both are approximations to a third theoretically correct form different from either, presumably more closely related to the Helmholtzian function.

V. Comparison with the Original Results of Helmholtz

Curve $R'''G'''B'''$ in Fig. 1 illustrates the approximate position of the spectral locus in the color triangle given by Helmholtz.[14] At first it was supposed the Helmholtzian primaries would require only minor readjustment to bring about best agreement of Eq. (2) with experimental data, and the spectral curve was allowed to occupy a similar position in the x_i triangle, with disappointing results. The corresponding derived curve of the Fig. 2 type ($d\lambda/dE$ plotted against λ) rose steeply from about λ480 mμ on toward the short wave end of the spectrum (Helmholtz did not carry this curve beyond λ480 mμ, lacking the necessary experimental data); and in addition, besides other lesser vagaries, exhibited an abrupt dip at about λ530 mμ approximately as deep as the major minima. At this wave-length Helmholtz likewise recorded a large deviation in his computed results, but attributed it to interpolative error, an exceptionally long gap in the meager experimental data at his disposal having occurred just here, and neglected the divergent result. The fact is, however, that the spurious minimum does exist, and it was found to persist so long as the

[14] H. v. Helmholtz, *Handbuch der Physiolog. Optik*, second edition, pp. 444–458.

spectral locus in the x_i triangle at all resembled that of the Helmholtz color triangle. Moreover, the derived curve of the same type as those of Fig. 3 (numbers of purity-change steps from "white" to spectral hues) bore little semblance to the latter, but had two minima, one in the yellow and another in the blue.

When it had become apparent that no material improvement could be hoped for with the spectral curve in this general position, the search was widened. Color chart *RGBW*, the eventual outcome, is obviously entirely unrelated to the solution found by Helmholtz. This result was arrived at by using only the two types of experimental data mentioned in the preceding paragraph, i.e. $d\lambda/dE$ along the spectrum, and purity-step counts; the agreement with the data represented in Figs. 4, 5 and 6 did not appear until after the final position of the spectral curve had been established, hence serves to confirm the result. This position is sharply defined as it accords with the existing data. No more than relatively slight changes can be made without appreciably impairing the agreement in some particular. The numerical coefficients in Eqs. (3A) are thus determined with considerable certainty, but since they are subject to readjustment as new data are acquired or upon the discovery of an improved form of line element, numerical evaluation of their precisions, which would be somewhat involved, has not been undertaken.

VI. Conclusions

Helmholtz'[14] derivation of Eqs. (1) and (2) is predicated upon three explicit assumptions in regard to the nature of the color-sense mechanism, which may be briefly stated as follows:

(1) There are three specific sensations of color.

(2) Each elementary color sensation individually conforms to the Weber-Fechner principle, which states, that over a middle range of intensities, sensation intensity varies as the logarithm of excitation intensity.

(3) The aggregate effect upon the visual consciousness of changing the intensities of more than one elementary color sensation at a time is given by the square root of the sum of the squares of the separate effects due to each sensation alone.

The success of Eq. (2) in coordinating measured chromatic thresholds with spectral mixture data, now demonstrated for the first time, thus automatically lends support to each of these hypotheses. Certainly it may now be said that a color-sense mechanism so constituted could possibly yield chromaticity-sensibility data much like the observed data of this sort now on record. This is obviously not to say, however, that the present result is susceptible of no other interpretation than that prescribed by the precise terms of Helmholtz' initial postulates.

In formulating the third of the above postulates, Helmholtz sought to find a function which would express as nearly as possible the expected end effect due to several superposed sensations of like type but distinct quality. He pointed out that the root-of-summed-squares relation proposed by him did not present an exact parallel, but had properties similar to the required. This "extention of the Weber-Fechner principle," so-called by Helmholtz, now receives its first direct substantiation based on experimental measurements. Judging from the present result, it offers an acceptable working approximation to actuality.

Equations (3A) define three "natural primaries," represented in the trilinear diagram of Fig. 1 by the apices of the x_i triangle. These three colors are all virtual rather than real, in the sense that they lie outside the gamut of colors actually seen. It now seems probable that these primaries (or others to which these approximate) correspond either directly or through some simple relationship to three elementary sensations of color. The interpretation placed upon them by the unmodified Helmholtzian theory is that they correspond directly to elementary sensations. Direct correspondence does not appear inevitable, however, and in fact there is some reason to anticipate an indirect connection.

Despite the essentially positive character of the present result, certain conflicts of a fundamental nature nevertheless occur, as already implied, between the color system defined by Eqs. (3A) and the theoretical considerations underlying Helmholtz' derivation of Eq. (2). Having established a color space in which Eq. (2) holds, then, were Helmholtz' assump-

tions[15] wholly correct, the universal line element, Eq. (1), from which Eq. (2) is derived, should likewise hold in this space, and hence on planes of uniform brightness in it should give the same results as Eq. (2). The consequences of Eq. (1) have been explored on a plane of uniform brightness in the color space defined by Eqs. (3A), and found to differ from those of Eq. (2). The fact that one of the primaries defined by Eqs. (3A) has a negative luminosity coefficient is also at variance with the initial postulates.

These discrepancies both alike apparently have to do primarily with the brightness phase of visual sensation, and suggest that the concept of brightness incorporated in the classical trisensational theory may have to be modified. The discrepancies could be explained, for instance, by assuming independent perception of the brightness and chromaticity attributes of visual sensation, an assumption, as Troland[16] has shown, many varied visual phenomena seem to support. But since this assumption introduces a somewhat radical departure from the classical theory, it will not be advanced for the present, pending examination of its full consequences by methods similar to those used in this research; and because of the uncertainty thus engendered, neither will a specific interpretation of the primaries here established be offered at this time.[17]

The writer cannot conclude without further acknowledgment of his very great debt to Dr. Deane B. Judd, whose valuable treatise has been drawn upon without reserve, and whose cooperation during the preparation of this and the preceding paper of this series has been most helpful.

[15] Cf. Helmholtz, reference 14. The derivation of Eq. (2) from Eq. (1) involves a tacit assumption with respect to the intrinsic nature of "brightness." Unless this holds, the two are not necessarily equivalent.

[16] L. T. Troland, J. O. S. A. **6**, 3 (1922).

[17] Since completion of this paper, a new general colorimetric line element has been proposed by Silberstein (L. Silberstein, J. O. S. A. **28**, 63 (1938)). Starting from considerations similar to those used by Helmholtz, Silberstein arrives at a different and much more complex function. This is not an appropriate place to comment on Silberstein's result beyond calling attention to the fact that his expression is not in the same category with that of Helmholtz in that its independent variables refer to arbitrarily chosen primary colors, the expression supposedly holding irrespective of the choice of primaries so long as these meet certain broad specifications. In view of the demonstrated agreement of the Helmholtzian function with observed data for the primaries established here, Silberstein's elaborate expression might be expected to reduce to some comparable form for these primaries, but it is not evident how this would occur.

Surrounding Gaseous Medium and the Herschel Effect

MARLIN THURSTON AND JULIAN M. BLAIR
University of Colorado, Boulder, Colorado

(Received June 18, 1938)

A. S. VNUKOVA[1] has predicted on theoretical grounds and has observed on Russian diapositive plates that the Herschel effect is accelerated in atmospheres of oxygen, is almost absent in atmospheres of carbon dioxide, and is replaced by the normal photographic blackening in atmospheres of hydrogen.

In attempting to repeat this work we have been unable to purchase any of the Russian plates but have gathered rather extensive data on other emulsions. A sheet was cut from a roll of Convira O paper, and longitudinal strips of it were given increasing exposures to the unfiltered radiation from a 60 w Mazda lamp, producing the densities shown at $t=0$ in Fig. 1. The Herschel effect was then produced by exposing transverse strips of the sheet while in an atmosphere of hydrogen to the radiation from a 400 w Mazda lamp at a distance of 60 cm filtered through a yellow 105 Schutzfilter. The sheet was then developed in metol-hydroquinone and finished as usual. The densities were measured with a very accurate photoelectric densitometer and in Fig. 1 are plotted against the time of exposure to the bleaching radiation. Other sheets were tested in an atmosphere of oxygen, and others in air.

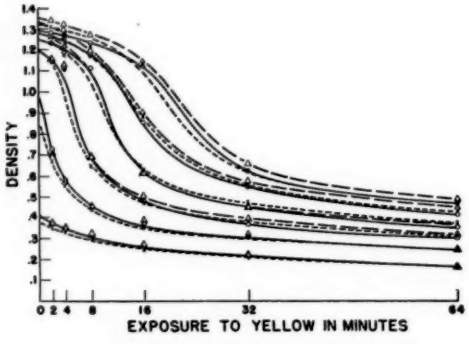

FIG. 1. Showing the rate of the Herschel effect in various gaseous atmospheres. Density is plotted against the time of exposure to the bleaching radiation. The Herschel effect in hydrogen is shown by the crosses and the dotted lines, in oxygen by the circles and the solid lines, and in air by the deltas and the dashed lines.

In other tests the sheets remained in an evacuated bell jar for 12 hours before the gases were introduced, and stood in the gases for 6 hours before the exposures were made. Other tests were made with Azo emulsions coated on glass, with bromide paper, and with Eastman positive motion picture film (a rather pure bromide emulsion).

All of these data suggest that under these conditions and on these emulsions the rate of the Herschel effect is not appreciably influenced by the presence of the various gases mentioned.

[1] A. S. Vnukova, Nature **138**, 246 (1936) also J. Phys. Chem. U. S. S. R. **9**, 598 (1937).

A Physical Density Comparator*

MONROE HAMILTON SWEET
Weston Electrical Instrument Co., Newark, New Jersey
(Received July 23, 1938)

INTRODUCTION

THE densitometer described below is the result of efforts to obtain a device which would surmount the shortcomings of existing commercial types. It was purposely constructed to fulfill the rather rigid requirements set forth by color-separation photography where it is desirable to measure accurately the densities of small areas of the separation negatives and positives.

An ideal instrument of this sort should be: (1) Direct reading, (2) objective in action, (3) accurate to at least 1 percent, (4) capable of measuring transmission and reflection densities, of areas of the order of $\frac{1}{64}''$ diameter (both specular and diffuse), (5) capable of measuring densities up to at least 3.0 without heating the film or paper under test, (6) capable of measuring directly, the density-differences of large absolute values.

DESIGN

With these points in view, a densitometer was constructed. Figs. 1 and 2 show the plan. Radiation from lamp *A* passes through the infrared absorbing liquid *W*; is then refracted by air-lens *B* so to be converged; and is further refracted upon leaving the liquid at *C*. It is then incident upon plane mirror *D*, and after passing through the fixed Polaroid[1] plate *E*, encounters the rotatable Polaroid plate *F* which will transmit a portion of the flux incident upon it, according to its angular position relative to *E*. Thereupon the flux is concentrated by condenser *G* so as to pass through the aperture *V* of aperture disk *H*, the blue component of a Viscor[2] filter *I*, the portion of the film under test *J*, and finally impresses itself on the Photronic[3] photoelectric cell *P*.

In use the plane of polarization of plate *F* was brought parallel to that of plate *E*, and with the film in place the photoelectric response of *P* was noted from a microammeter (not shown). After the film was removed, plate *F* was rotated by means of index *M* until a response resulted equal to the original. The scale of the index *S* was calibrated directly in terms of density units. It may also be calibrated to read directly, in terms of transmission, relative exposure units, or any other functional unit which is most convenient for the particular application at hand.

In Fig. 3, curve 1 shows the relationship of the angle between the planes of polarization of the two superposed Polaroid plates to the resulting

[1] M. Grabau, J. O. S. A. **12**, 420 (1937).
[2] H. P. Gauge, J. O. S. A. **4**, 159 (1937).
[3] Weston Electrical Instrument Corporation, Technical Data Bulletin No. B-18-A.

* Patents pending.

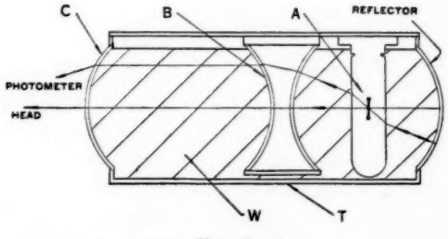

FIG. 1.

A, Light source
B, Air lens
C, Exit window
D, Plane mirror
E, Fixed Polaroid plate
F, Rotatable Polaroid plate
G, Condensing lens
H, Aperture disk
I, Blue filter
J, Film under test
M, Index
P, Photronic photo-cell
Q, Plane glass plate

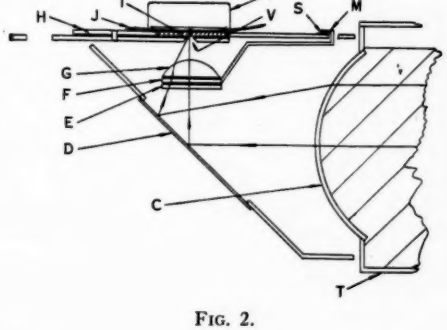

FIG. 2.

S, Scale
T, Tank
V, Aperture
W, Liquid (generally water)
YV, Yellow filter
C_2, Condenser.

density (with the density subtracted for the condition when the planes of polarization are parallel). Because plate F must be rotated through a relatively large arc to determine a small density difference, the instrument is especially well suited to the measurement of minute density differences of two or more portions of the film. This is accomplished by interposing the denser portion between the cell and the mask, and noting the galvanometer response with the planes of polarization parallel, thereupon replacing the denser section with the thinner and rotating the adjustable plate until the galvanometer response is the same. Then the position of the index indicates the density difference between the two sections.

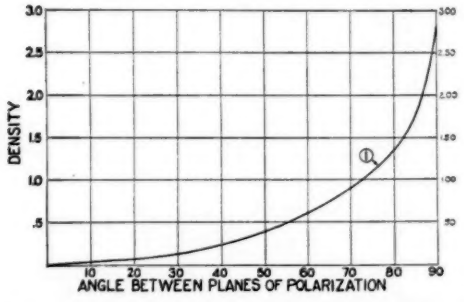

FIG. 3. The resultant density of the superposed Polaroid plates as a function of the angle between their planes of transmission, plotted from experimentally observed results.

For measuring reflection coefficients, the optical system illustrated in Fig. 4 was used. The surface to be tested was held in position against plane glass Q by the pressure plate. The galvanometer response was noted and the test surface was replaced with a standard surface whose reflection density was known to be approximately zero. The index was adjusted for the same galvanometer response and since the same scale was used as for transmission densities, the index read reflection density values directly. Plane glass Q, was located at such an angle that flux specularly reflected by it would not encounter condenser C_2. The yellow component of a Viscor filter was here introduced at YV in addition to the blue filter mentioned above because in this type of measurements we were primarily concerned with visual effects rather than actinic ones as elsewhere.

General Discussion of Experimental Technique

The fixed Polaroid E is so oriented that (as shown) its plane of polarization is at right angles to the plane of the paper. This is desirable because if slight polarization is introduced at the plane mirror D, the intensity of the flux transmitted by the fixed plate will then not be reduced. For the liquid W, water has been found to be most suitable† because of its excellent optical[4] and thermal characteristics. The use of Polaroid plates, the photronic cell, and very small apertures, all contribute to the necessity for obtaining extremely high flux concentrations from whose spectrum the infra-red portion has been abstracted. This has been accomplished in the present design.

The optical qualities of Polaroid have been described by M. Grabau.[1] However, there is one characteristic pertinent to the present application not mentioned by him. This characteristic results in the fact that when two plates are oriented for extinction for light parallel to the optic axis, transmission will occur for light incident at angles other than normal and increasingly so as the angle is increased. This means that ideally all of the flux used should be passed through the plates parallel to the optic axis and be condensed thereafter. The instrument was so designed that the maximum angle of incidence of light upon the plates was 17°. Tests seemed to indicate that angles up to this value are permissible. To the best of the writer's knowledge no quantitative

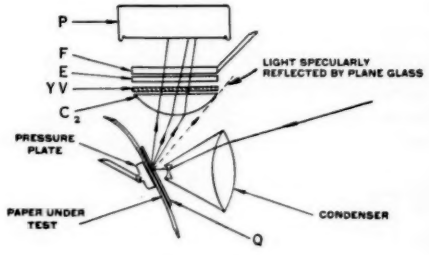

FIG. 4.

† A 2.5 percent solution of cupric chloride may be used where even greater infra-red absorbtion is desired. It will tend to correct the tungsten radiation to approximate daylight.

[4] Coblentz, Bull. Bur. Standards 619 (1911).

data have yet been published concerning the incomplete polarization of light incident at angles other than normal.

In the following equations H_p represents the extinction factor‡ of the superposed Polaroid plates when their planes of polarization are parallel; H_x the extinction factor when their planes are crossed. The quotient $(H_p/H_x)_\lambda$ vs. λ is shown[5] by curve 2, Fig. 5. The function P is the relative response of the Photronic[3] cell and is plotted against λ in curve 5, Fig. 6. Similarly curve 4, Fig. 6, shows the spectral distribution of radiant flux (T_λ) of the light source plotted against λ for tungsten at 3000°K. Curve 3, Fig. 6, is plotted as F vs. λ where F is the relative transmission of the blue component of the Viscor filter.[2] The curve $(H_p/H_x)_\lambda$ vs. λ (Fig. 5) is plotted in relative values.

We are interested in the ratio of the total photoelectric response for the condition when the planes of polarization are parallel to the response when the planes are crossed. Let this function be termed "Resultant Relative Response."§ Using the symbols given above, the function assumes the form:

$$\text{R. R. R.} = \frac{\int_{\lambda=0}^{\lambda=\infty} (H_p)_\lambda (T)_\lambda (F)_\lambda (P_\lambda) d\lambda}{\int_{\lambda=0}^{\lambda=\infty} (H_x)_\lambda (T)_\lambda (F)_\lambda (P)_\lambda d\lambda}.$$

For this particular group of constituent materials used, the numerical value of this expression was experimentally found to be 630. As a matter of comparison, the blue filter was then removed so that the expression assumes the form:

$$\text{R. R. R.} = \frac{\int_{\lambda=0}^{\lambda=\infty} (H_p)_\lambda (T)_\lambda (P)_\lambda d\lambda}{\int_{\lambda=0}^{\lambda=\infty} (H_x)_\lambda (T)_\lambda (P)_\lambda d\lambda}.$$

With the remaining materials and conditions the same as before the experiment showed the numerical value now to be 40. The difference between the results obtained, demonstrates the increased operating sensitivity of the device when using the blue filter.

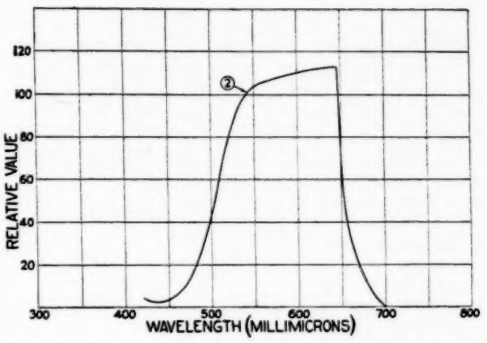

FIG. 5. The "extinction factor" for Polaroid plates as a function of wave-length. (Calculated values.)

The blue filter mentioned above was used primarily in order to work within the spectral range where Polaroid is most effective as a polarizing agent. Fortunately, the bromides and chloro-bromides are also more sensitive in the blue portion of the spectrum so that when using the densitometer for the determination of photographic printing times the results obtained with the blue filter interposed are more valid than those obtainable with visual types of densitometers. This is especially true in the event that the films are stained during processing as shown in the following example. The fog density of an unexposed section of 35 mm film[6] which had been developed in a paraphenylenediamine developer[7] (and consequently stained reddish-brown), was found to be 0.05 when measured by a commercial densitometer.[8] Subsequent measurements on the present comparator|| showed it to have an effective density of 0.45. In order to clarify this discrepancy, the contact printing density of this film was measured as follows:

A strip of bromide projection printing paper[9]

‡ The handling of the problem is clarified by regarding the transmission of the plates as "extinction factor."

[5] The data from which this curve was plotted are given by M. Grabau, reference 1.

§ Because water is nearly perfectly transparent throughout the spectral region to which the Photronic cell is sensitive, its action as a filter for actinic flux is not considered.

[6] Agfa Supersensitive miniature camera film.

[7] Marketed under the trade name "M. P. G." and distributed by the R. J. Fitzsimmons Corporation, N. Y.

[8] The Eastman "Capstaff-Purdy" densitometer.

|| The two densitometers were previously found to be in excellent agreement for density measurements of neutral subjects.

[9] Defender Velour Black Surface *A* normal, developed in Eastman D-72 (strength 1 : 2), for two minutes at 65°F.

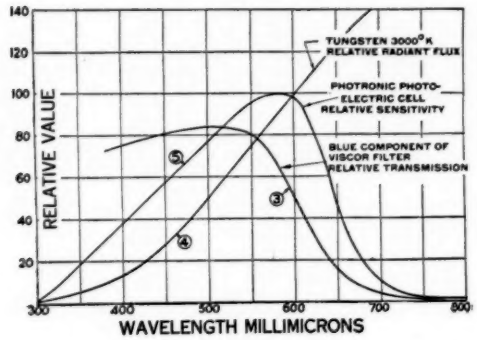

FIG. 6. Curve 3—The transmission of the blue filter *versus* wave-length. Curve 4—Relative radiant flux for tungsten at 3000°K plotted against wave-length. Curve 5—Current response of the photronic cell *versus* the wave-length of incident light.

was exposed under a 2.4 flashlight lamp operating from a 6 volt storage battery, and with sufficient series resistance to reduce the filament current to 0.63 ampere. The strip was placed at a distance of 24.5 inches from the plane of the filament and five sections were exposed, with no film interposed for 18, 22, 27, 33, and 40 seconds respectively.

At the same distance from the light source two portions of the strip were then exposed through the fog section of the film for 27 and 62 seconds, with the other conditions unchanged.

Figure 7 shows the results. Inspection reveals that the density corresponding to the 62-second exposure through the film is closely matched with that corresponding to the 22-second exposure of the standard series. For the matched condition, the contact printing density of the film is $D = \log_{10}(t/T)$ where t is the exposure time for the test block and equals 62 seconds; T is the exposure time for the standard and equals 22 seconds. Substituting these values we get 0.45 as the real film density. This validated the previous measurement made with the densitometer here described.

As has been clearly demonstrated by Tuttle[10] and others, there are so many different optical arrangements in common use in connection with photographic printing that in arriving at an expression of accuracy of density measurements the exact optical system must be specified if the results are to be of much use. Nevertheless, it is interesting to note that with the comparator here described no observable inconsistency could be detected in the measurements of homogeneous areas through apertures of various sizes and at different times.

As constructed, the instrument measured diffuse density. However, there exists a definite function[11] such that when the diffuse density

FIG. 7. Copy of a test strip printed on a bromide paper. The numbers in the blocks of the graduated series of density steps represent the times (in seconds) to which each step was exposed to a standard light source. The two blocks at the top of the strip were exposed through a selected section of a 35 mm film to the same source for the indicated durations. The block which was exposed for 62 seconds was based on a measurement made with the present densitometer. The block which was exposed for 27 seconds was based on a measurement made with a conventional commercial densitometer. Both exposure times were so calculated from these measurements that the resulting print densities should have been equal to that step of the graduated series which had been exposed to the standard lamp for 22 seconds.

[10] A. M. Koerner and Clifton Tuttle, J. O. S. A. **7**, 241 (1937).

[11] Known as "Callier's coefficient." For a recent investigation of this subject see C. Tuttle, J. O. S. A. and Rev. Sci. Inst. **12**, 559 (1926).

values are multiplied by this function, specular values or intermediate values between specular and diffuse result. This function can be calibrated into the scale and the instrument be made to read directly in terms of the desired units.

Summary

A density comparator was constructed using filtered tungsten radiation and Polaroid plates as a means for obtaining an accurate standard of comparison. In order to measure the densities of small areas of the negatives and print, high flux concentrations were used. The infra-red was filtered from the total radiation by submerging the incandescent source in a tank of water. A water-air lens was used to condense the light. The instrument permitted the measurement of both transmission and reflection densities.